PHYSICAL REVIEW D VOLUME 23, NUMBER 12 15 JUNE 1981

Strong-coupling expansion for the effective potential on a lattice

Carl M. Bender
Department of Physics, Washington University, St. Louis, Missouri 63130

Fred Cooper and Gerald S. Guralnik*
Theoretical Division, Los Alamos Scientific Laboratory, Los Alamos, New Mexico 87545

Ralph Roskies
Department of Physics, University of Pittsburgh, Pittsburgh, Pennsylvania 15260

David H. Sharp
Theoretical Division, Los Alamos Scientific Laboratory, University of California, Los Alamos, New Mexico 87545
(Received 2 February 1981)

This is the first of three papers on the strong-coupling expansion of the renormalized effective potential in $g\phi^4$ quantum field theory in d-dimensional Euclidean space-time. In this paper we show how to express the effective potential in terms of one-particle-irreducible strong-coupling graphs. We describe two methods for obtaining analytic expressions for the vertices of these graphs. We also present an algebraic technique for evaluating the graphs on a Euclidean space-time lattice in arbitrary dimension d.

I. INTRODUCTION

In a recent letter[1] we reported some numerical and analytical results on the renormalized effective potential in $g\phi^4$ field theory in the strong-coupling limit. Here and in the following two papers we present the detailed results of this investigation and give a thorough treatment of the calculational procedures. Roughly speaking, our calculations consist of (1) obtaining the unrenormalized lattice strong-coupling series for the effective potential, (2) performing a mass and wave-function renormalization of this series, and (3) taking the continuum limit of this series by extrapolating to zero lattice spacing. The renormalized strong-coupling expansion that we obtain in the continuum is a series in powers of the dimensionless parameter M^{4-d}/g, where M is the renormalized mass and g is the bare coupling constant. The calculations we describe here are done in a Euclidean space-time of arbitrary dimension d. Our objective is to obtain detailed numerical results for the first four coefficients of the effective potential and the β function. These numerical results are given in the second and third papers of this series.

In this paper we concentrate on the analytical machinery necessary to derive the lattice strong-coupling expansions of a field theory with polynomial interaction $P(\phi^2)$ in d-dimensional space-time. Although we focus on $g\phi^4$ theory our methods extend trivially to theories having more general polynomial interactions.

Our starting point is the vacuum-persistence functional $\langle 0_+ | 0_- \rangle_J$ in the presence of an external source J:

$$\langle 0_+ | 0_- \rangle_J = Z[J] = N \int \mathfrak{D}\phi \exp\left\{ -\int d^dx [(\partial\phi)^2/2 + m^2\phi^2/2 + g\phi^4/4 - J\phi] \right\}, \tag{1.1}$$

where N is a normalization factor independent of J which makes $Z[0] = 1$. The connected Green's functions $W_n(x_1, x_2, \ldots, x_n)$ of the theory are computed from $Z[J]$ in (1.1) by taking functional derivatives with respect to the external source:

$$W_n(x_1, \ldots, x_n) = \frac{\delta}{\delta J(x_1)} \cdots \frac{\delta}{\delta J(x_n)} \ln Z[J] \Big|_{J=0}. \tag{1.2}$$

Later in this section we show how to derive a set of graphical rules for the lattice strong-coupling expansion of the Green's functions of the theory. The graphs in this expansion are organized by the number of free inverse propagators $D^{-1}(x, y) = \partial^2 \delta(x - y)$; this is in contrast with the conventional weak-coupling expansion whose graphs are organized by the number of bare vertices. The Green's functions are obtained by summing over all graphs, the contribution of each graph being the product of its vertices, its symmetry number, and the value obtained by integrating over the positions of the internal vertices.

In Sec. II we give a detailed derivation of the vertices of the lattice diagrams. In fact, we give *two different* strong-coupling expansions of the vertices, valid in different regions of bare parameter space, the first one for fixed m^2 and the second one for large negative m^2. In a previous paper[2] we used the first vertex expansion to solve for the energy eigenvalues of the anharmonic os-

cillator as a series in powers of $m^2/g^{2/3}$. A preliminary discussion of the second vertex expansion was also given recently.[3] Here we compute the effective potential using both vertex expansions and in the second paper of this series we give detailed numerical comparisons of the continuum extrapolations of the two series.

In Sec. III we give a very simple algebraic procedure for evaluating graphs (summing over the positions of all internal vertices) on a d-dimensional hypercubic lattice. We find that the vacuum graphs, which are important because they determine the effective potential, have a very simple form: every graph having n lines D^{-1} is a polynomial in the dimension d of degree n. Thus, we have a very simple analytic continuation of the lattice theory to arbitrary complex dimension d. In the Appendix we discuss the connection between our results and the way results are usually presented in statistical mechanics calculations.

In Sec. IV we show how to express the effective potential in terms of one-particle-irreducible graphs, where in strong-coupling expansions one-particle irreducibility refers to the lines representing the free inverse propagator D^{-1}. We conclude this paper by displaying two unrenormalized lattice strong-coupling expansions for the effective potential, one for each vertex expansion. The first expansion is a double series in powers of the parameters

$$\epsilon = (ga^{4-d})^{-1/2} \text{ and } s = m^2a^2,$$

where a is the lattice spacing. The second expansion is also a double series in powers of $\alpha = -m^2a^{d-2}/g$ and $\delta = gm^{-4}a^{-d}$.

We conclude this section by briefly recalling the derivation of the graphical rules for evaluating Green's functions on the lattice. We rewrite (1.1) formally as

$$Z[J] = \exp\left(\tfrac{1}{2}\int d^dx \int d^dy\, D^{-1}(x-y)\frac{\delta}{\delta J(x)}\frac{\delta}{\delta J(y)}\right)Z_0(J), \tag{1.3}$$

where

$$Z_0[J] = N\int \mathfrak{D}\phi \exp\left[-\int d^dx(m^2\phi^2/2 + g\phi^4/4 - J\phi)\right]. \tag{1.4}$$

From (1.3) we read off the bare propagator $D^{-1}(x-y) = \partial^2\delta(x-y)$ for the graphs of the theory. In order to calculate graphs on a lattice we interpret $D^{-1}(x-y)$ as its lattice counterpart in terms of Kronecker δ functions [see (3.2)]. The vertices of the theory are obtained from $Z_0[J]$ in (1.4) using two different series expansions in the next section.

II. EVALUATION OF THE VERTICES

To obtain the vertices of the theory from $Z_0[J]$ in (1.4) we first write $Z_0[J]$ as a product of ordinary integrals on a lattice:

$$Z_0[J] = N' \prod_{\substack{\text{all lattice}\\ \text{points } i}} \frac{F(J_i)}{F(0)} = N' \exp\left(\sum_i \ln\frac{F(J_i)}{F(0)}\right), \tag{2.1}$$

where $F(y)$ is an ordinary one-dimensional integral

$$F(y) = \int_{-\infty}^{\infty} \exp[-a^d(m^2x^2/2 + gx^4/4 - yx)]dx \tag{2.2}$$

and N' is a new normalization constant independent of J. To derive (2.1) we use the definition of the path integral as a limit of a lattice structure in which we have made Euclidean space-time discrete:

$$x = ai,$$
$$\phi(x) = \phi(ai) = \phi_i,$$
$$\frac{d\phi(x)}{dx} = (\phi_{i+1} - \phi_i)/a,$$
$$\int_{-\infty}^{\infty} d^dx\, \phi(x) = a^d \sum_i \phi_i,$$
$$\int \mathfrak{D}\phi(x) = \lim_{\substack{a\to 0,\\ x=ai}} \prod_i \int d\phi_i \cdot$$

To compute the vertices we first expand $F(y)/F(0)$ as a power series in y:

$$\frac{F(y)}{F(0)} = \sum_{n=0}^{\infty} \frac{A_{2n}y^{2n}}{A_0(2n)!}, \tag{2.3}$$

where

$$A_{2n} = \int_{-\infty}^{\infty} dx(xa^d)^{2n}\exp[-a^d(gx^4/4 + m^2x^2/2)]. \tag{2.4}$$

The A_{2n}/A_0 are the disconnected vertices of the theory. To obtain the usual connected $2n$-point vertices L_{2n} we must expand the logarithm of (2.3):

$$\ln\frac{F(y)}{F(0)} = \sum_{n=0}^{\infty} \frac{L_{2n}}{(2n)!}y^{2n}. \tag{2.5}$$

This result was discussed at length in Ref. 2 with the difference that the bare mass term was not included in (2.4) but was instead included in the definition of $D^{-1}(x-y)$.

First method for expanding vertices

The two expansions of the vertices that we referred to earlier originate from the two different ways of evaluating the integral in (2.4) in the large-g regime. The first method consists of expanding the integrand of (2.4) in powers of m^2 and then integrating term by term. This produces the following series for A_{2n}:

$$A_{2n} = a^{2nd}\left(\frac{4}{ga^d}\right)^{n/2+1/4}\sum_{l=0}^{\infty}\frac{(-s\epsilon)^l}{l!}\Gamma\left(\frac{n}{2}+\frac{1}{4}+\frac{l}{2}\right), \tag{2.6}$$

where s and ϵ are dimensionless variables defined by

$$s = m^2a^2, \quad \epsilon = (ga^{4-d})^{-1/2}. \tag{2.7}$$

From (2.3), (2.5), and (2.6) we obtain the first eight vertices

$$\begin{aligned}
L_2 &= 2R\epsilon + (4R^2-1)s\epsilon^2/2 + 2R^3s^2\epsilon^3 + (48R^4-1)s^3\epsilon^4/24 + (96R^5-R)s^4\epsilon^5/48 + (80R^6-R^2)s^5\epsilon^6/40 \\
&\quad + (480R^7-7R^3)s^6\epsilon^7/240 + (80\,640R^8-1344R^4+5)s^7\epsilon^8/40\,320 + \ldots, \\
L_4 &= (-12R^2+1)\epsilon^2 + (-24R^3+4R)s\epsilon^3 - (144R^4-16R^2+1)s^2\epsilon^4/4 - (96R^5-8R^3-R)s^3\epsilon^5/2 \\
&\quad - (720R^6-48R^4-9R^2+1)s^4\epsilon^6/12 - (8640R^7-480R^5-126R^3+5R)s^5\epsilon^7/120 \\
&\quad - (80\,640R^8-3840R^6-1344R^4+48R^2+5)s^6\epsilon^8/960 + \ldots, \\
L_6 &= (240R^3-24R)\epsilon^3 + (720R^4-144R^2+5)s\epsilon^4 + (1440R^5-264R^3+17R)s^2\epsilon^5 \\
&\quad + (2400R^6-384R^4+2R^2)s^3\epsilon^6 + (14\,400R^7-2016R^5-82R^3+21R)s^4\epsilon^7/4 \\
&\quad + (1\,209\,600R^8-149\,760R^6-12\,480R^4+1872R^2-85)s^5\epsilon^8/240 + \ldots, \\
L_8 &= (-10\,080R^4+1344R^2-30)\epsilon^4 + (-40\,320R^5+9408R^3-492R)s\epsilon^5 \\
&\quad + (-100\,800R^6+24\,192R^4-2004R^2+40)s^2\epsilon^6 + (-201\,600R^7+45\,696R^5-2676R^3+68R)s^3\epsilon^7 \\
&\quad - (2\,822\,400R^8-591\,360R^6+16\,704R^4+3040R^2-65)s^4\epsilon^8/8 + \ldots,
\end{aligned} \tag{2.8}$$

$$\begin{aligned}
L_{10} &= (725\,760R^5-120\,960R^3+4632R)\epsilon^5 + (3\,628\,800R^6-967\,680R^4+69\,072R^2-960)s\epsilon^6 \\
&\quad + (10\,886\,400R^7-3\,144\,960R^5+319\,992R^3-10\,440R)s^2\epsilon^7 \\
&\quad + (25\,401\,600R^8-7\,257\,600R^6+681\,792R^4-28\,320R^2+375)s^3\epsilon^8 + \ldots, \\
L_{12} &= (-79\,833\,600R^6+15\,966\,720R^4-877\,536R^2+9120)\epsilon^6 \\
&\quad + (-479\,001\,600R^7+143\,700\,480R^5-12\,922\,272R^3+333\,840R)s\epsilon^7 \\
&\quad + (-1\,676\,505\,600R^8+558\,835\,200R^6-67\,402\,368R^4+3\,063\,072R^2-29\,550)s^2\epsilon^8 + \ldots, \\
L_{14} &= (12\,454\,041\,600R^7-2\,905\,943\,040R^5+208\,143\,936R^3-4\,284\,000R)\epsilon^7 \\
&\quad + (87\,178\,291\,200R^8-29\,059\,430\,400R^6+3\,141\,186\,048R^4-119\,048\,832R^2+887\,640)s\epsilon^8 + \ldots, \\
L_{16} &= (-2\,615\,348\,736\,000R^8+697\,426\,329\,600R^6-61\,578\,316\,800R^4+1\,918\,393\,344R^2-11\,503\,440)\epsilon^8,
\end{aligned}$$

where $R = \Gamma(\frac{3}{4})/\Gamma(\frac{1}{4}) = 0.337\,989\,120$.

It is important to notice that the order-ϵ^n contribution to the graphs for the $2k$-point Green's function contains exactly $n-k$ internal lines D^{-1} connecting vertices L_{2m} with $m \leq n$. Thus, the power of ϵ counts the number of D^{-1} lines in the graph; that is, organizing the graphs in powers of ϵ is exactly equivalent to organizing the graphs in powers of D^{-1} or numbers of internal lines. This can be seen clearly from Figs. 1 and 2 of Ref. 2. Furthermore the power of the parameter s counts the number of m^2 mass corrections to the zero-bare-mass theory.

Second method for expanding vertices

The previous expansion has a defect from the point of view of renormalization theory. For example, for the anharmonic oscillator ($d=1$) one finds that in the limit $g \to \infty$, $a \to 0$, m fixed, the renormalized mass M (defined, say, as the lowest pole of the two-point Green's function) approaches ∞ as $g^{1/3}$. However, in field theory we wish to allow g to tend to ∞ keeping M fixed. In this limit the anharmonic potential becomes a double well and m^2 tends to $-\infty$. This violates the original assumption (that m^2 can be held fixed)

which was used to derive the expansion in (2.6). In the second paper in this series we will see that the renormalized extrapolants for the renormalized effective potential which are based on the method-1 vertices in (2.8) converge slowly. We presume that this slow convergence is due to the above problem.

One can use a mean-field calculation to estimate the growth of m^2 as $g \to \infty$ with M held fixed in a d-dimensional quantum field theory. The leading mean-field approximation to the gap equation is[4]

$$M^2 = m^2 + \frac{g}{(2\pi)^d}\int \frac{d^dk}{k^2+M^2} .$$

Thus, for fixed M^2, we have for $d < 2$

$$m^2 \sim -gM^{d-2} \quad (g \to \infty) .$$

In the regime of large negative mass we evaluate the integral representation for A_{2n} in (2.4) by Laplace's method of moving maxima. We notice that $gx^4/4 + m^2x^2/2$ has a vanishing derivative at $x_0 = (-m^2/g)^{1/2}$. To keep this minimum at a fixed value of x we let

$$m^2 = -g\alpha a^{2-d} , \tag{2.9}$$

where α is a dimensionless parameter which, as we will see, counts the number of D^{-1} lines in graphs in the same way that ϵ does for the method-1 vertices in (2.8).

The simplest way to calculate the A_{2n} makes use of the formula

$$A_{2n} = \left(\frac{2a^{2d-2}}{g}\frac{d}{d\alpha}\right)^n I(\alpha) , \tag{2.10}$$

where

$$I(\alpha) = \int_{-\infty}^{\infty} dx \exp[-a^d g(x^4/4 - a^{2-d}\alpha x^2/2)] . \tag{2.11}$$

Laplace's method applied to (2.11) gives

$$I(\alpha) = 2(g\alpha)^{-1/2}e^{\delta/4}\left(1 + \tfrac{3}{4}\delta + \frac{105}{32}\delta^2 + \frac{3465}{128}\delta^3 + \frac{675\,675}{2048}\delta^4 + \frac{43\,648\,605}{8192}\delta^5 + \frac{7\,027\,425\,405}{65\,536}\delta^6 + \frac{677\,644\,592\,625}{262\,144}\delta^7 + \frac{609\,202\,488\,769\,875}{8\,388\,608}\delta^8 + \frac{78\,180\,986\,058\,800\,625}{33\,554\,432}\delta^9 + \frac{22\,563\,032\,576\,569\,860\,375}{268\,435\,456}\delta^{10} + \ldots\right)$$

$$= 2(g\alpha\pi)^{-1/2}e^{\delta/4}\sum_{n=0}^{\infty}\Gamma(2n+\tfrac{1}{2})\delta^n/n! , \tag{2.12}$$

where

$$\delta = gm^{-4}a^{-d} = \epsilon^2\alpha^{-2} . \tag{2.13}$$

Equation (2.12) is obtained easily by recognizing that (2.11) is the integral representation for the parabolic cylinder function $D_{-1/2}(m^2/\sqrt{2g})$. The series in (2.12), which is valid when g/m^4 is small for fixed a, is the asymptotic expansion of $D_{-1/2}$ for large negative argument. Similarly, (2.6) is the Taylor expansion of $D_{-1/2-n}$ for small argument. The weak-coupling series, not discussed here, corresponds to expanding $D_{-1/2}$ asymptotically for large positive argument.

From (2.10) and (2.12) we compute a series expansion for A_{2n} having the form $A_{2n} = \alpha^n$ (power series in δ). Finally, using (2.3) and (2.5) we obtain the following expansions for the first eight vertices L_{2n}:

$$L_2 = \alpha - \alpha\delta - 3\alpha\delta^2 - 24\alpha\delta^3 - 297\alpha\delta^4 - 4896\alpha\delta^5 - 100\,278\alpha\delta^6 + \ldots ,$$

$$L_4 = -2\alpha^2 + 6\alpha^2\delta + 12\alpha^2\delta^2 + 102\alpha^2\delta^3 + 1314\alpha^2\delta^4 + 22\,266\alpha^2\delta^5 + 464\,940\alpha^2\delta^6 + \ldots ,$$

$$L_6 = 16\alpha^3 - 72\alpha^3\delta - 96\alpha^3\delta^2 - 1008\alpha^3\delta^3 - 13\,824\alpha^3\delta^4 - 242\,712\alpha^3\delta^5 - 5\,187\,456\alpha^3\delta^6 + \ldots ,$$

$$L_8 = -272\alpha^4 + 1632\alpha^4\delta + 960\alpha^4\delta^2 + 18\,432\alpha^4\delta^3 + 270\,432\alpha^4\delta^4 + 4\,921\,344\alpha^4\delta^5 + 107\,640\,576\alpha^4\delta^6 + \ldots , \tag{2.14}$$

$$L_{10} = 7936\alpha^5 - 59\,520\alpha^5\delta + 9600\alpha^5\delta^2 - 552\,960\alpha^5\delta^3 - 8\,547\,840\alpha^5\delta^4 - 160\,807\,680\alpha^5\delta^5 - 3\,594\,792\,960\alpha^5\delta^6 + \ldots ,$$

$$L_{12} = -353\,792\alpha^6 + 3\,184\,128\alpha^6\delta - 2\,901\,504\alpha^6\delta^2 + 25\,576\,704\alpha^6\delta^3 + 399\,052\,800\alpha^6\delta^4 + 7\,733\,366\,784\alpha^6\delta^5 + 176\,431\,716\,864\alpha^6\delta^6 + \ldots ,$$

$$L_{14} = 22\,368\,256\alpha^7 - 234\,866\,688\alpha^7\delta + 390\,168\,576\alpha^7\delta^2 - 1\,767\,241\,728\alpha^7\delta^3 - 25\,846\,087\,680\alpha^7\delta^4 - 514\,502\,295\,552\alpha^7\delta^5 - 11\,962\,793\,816\,064\alpha^7\delta^6 + \ldots ,$$

$$L_{16} = -1\,903\,757\,312\alpha^8 + 22\,845\,087\,744\alpha^8\delta - 55\,084\,843\,008\alpha^8\delta^2 + 177\,421\,787\,136\alpha^8\delta^3$$
$$+ 2\,214\,464\,790\,528\alpha^8\delta^4 + 45\,277\,872\,390\,144\alpha^8\delta^5 + 1\,071\,598\,216\,937\,472\alpha^8\delta^6 + \ldots .$$

These L_{2n} are the method-2 analogs of the vertices in (2.8). In analogy with the variable ϵ, the power of α counts the number of D^{-1} lines and the power of δ counts the number of corrections to the $g \to \infty$ limit of the theory. The case $\delta = 0$ is referred to as the Ising field theory.[5]

III. ALGEBRAIC METHOD FOR EVALUATING d-DIMENSIONAL GRAPHS

In this section we describe a systematic algebraic technique for evaluating diagrams on a cubic Euclidean space-time lattice of arbitrary dimension d. We ignore here the contributions from the vertices because they are multiplicative constants which can be included after the graphs have been evaluated.

The basic line element from which all graphs are constructed is the inverse propagator $D^{-1}(x,y)$. In the continuum $D^{-1}(x,y)$ takes the form

$$D^{-1}(x,y) = \partial^2\delta(x-y). \tag{3.1}$$

Notation

On a lattice $D^{-1}(x,y)$ can be represented as a matrix. For example, on a one-dimensional lattice of lattice spacing a (3.1) becomes

$$D^{-1} = a^{-3}(\delta_{i,j+1} - 2\delta_{i,j} + \delta_{i+1,j}), \tag{3.2}$$

which may be formally represented as the one-dimensional matrix

$$D^{-1} = a^{-3}(1 \;\; -2 \;\; 1). \tag{3.3}$$

On a two-dimensional lattice D^{-1} is the two-dimensional matrix

$$D^{-1} = a^{-4}\begin{pmatrix} & 1 & \\ 1 & -4 & 1 \\ & 1 & \end{pmatrix}. \tag{3.4}$$

On a d-dimensional lattice D^{-1} and all other propagator graphs are quite cumbersome to represent using the above kind of matrix notation.

Thus, we introduce a more compact notation[6]:

(0) represents the position at the *center* of the d-dimensional matrix.

(1) represents the positions *one unit away* from the center of a matrix in all directions. Note that in a d-dimensional matrix there are $2d$ such positions, one unit up and one unit down each of the d axes.

(2) represents the positions two units away from the center of a matrix in all directions, up and down each of the d axes. There are $2d$ such positions.

(3) represents the $2d$ positions three units up and down each of the axes.

(11) represents the $2d(d-1)$ positions, one unit up or down each of two different axes.

(12) represents the $4d(d-1)$ positions, one unit up or down one axis and two units up or down a different axis.

(111) represents the $4d(d-1)(d-2)/3$ positions one unit up or down each of three distinct axes.

Using this notation we can represent the class of matrices that arises in the evaluation of propagator graphs on a lattice, specifically those matrices whose entries in the (1) positions, (11) positions, (12) positions, (2) positions, and so on, are all the same. For example, in one dimension, we represent the matrix (6, 3, −1, 3, 6) by 6(2) + 3(1) − (0). In two dimensions we represent the matrix

$$\begin{pmatrix} & & 3 & & \\ & 8 & 9 & 8 & \\ 8 & 7 & 6 & 7 & 8 \\ 3 & 9 & 6 & 2 & 6 & 9 & 3 \\ 8 & 7 & 6 & 7 & 8 \\ & 8 & 9 & 8 & \\ & & 3 & & \end{pmatrix}$$

by 3(3) + 8(12) + 7(11) + 9(2) + 6(1) + 2(0). In d dimensions, the matrix representation of D^{-1} is

$$D^{-1} = \frac{1}{a^{d+2}}[(1) - 2d(0)]. \tag{3.5}$$

Clearly, the advantage of this notation is that it reduces a d-dimensional matrix to a one-dimensional linear combination of vectors.

Parallel structures in propagator graphs—dot products

In the evaluation of propagator graphs (graphs having two external legs) the simplest structure involves repeated connections between two points. For example, in Fig. 1(a) we have *two* lines joining the two vertices in parallel. In one dimension, using a clumsy notation, we could evaluate the graph in Fig. 1(a) using (3.2):

$$\left[\frac{1}{a^3}(\delta_{i,j+1} - 2\delta_{i,j} + \delta_{i+1,j})\right]^2 = \frac{1}{a^6}(\delta_{i,j+1} + 4\delta_{i,j} + \delta_{i+1,j}).$$

We obtain this result using the fact that a Kron-

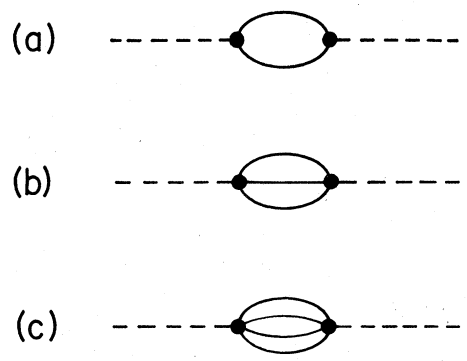

FIG. 1. Propagator graphs with repeated connections between two points.

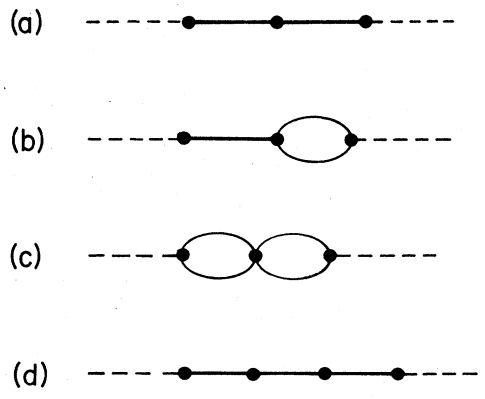

FIG. 2. Propagator graphs with series structures.

ecker δ is a projection operator: The product of two different Kronecker δ's vanishes and the square of a Kronecker δ equals itself.

To generalize this argument to d dimensions, we observe that the objects $\underline{(0)}$, $\underline{(1)}$, $\underline{(11)}$, $\underline{(2)}$, ... satisfy simple projective (orthonormal) dot product algebraic relations

$$\underline{(0)}\cdot\underline{(0)}=(0),\quad \underline{(1)}\cdot\underline{(1)}=\underline{(1)},\quad \underline{(11)}\cdot\underline{(11)}=\underline{(11)},\quad \underline{(2)}\cdot\underline{(2)}=\underline{(2)},\ldots \tag{3.6a}$$

and

$$0=\underline{(0)}\cdot\underline{(1)}=\underline{(1)}\cdot\underline{(11)}=\underline{(2)}\cdot\underline{(21)}=\underline{(2)}\cdot\underline{(0)}=\ldots. \tag{3.6b}$$

Now we represent the graph in Fig. 1(a) as the dot product $D^{-1}\cdot D^{-1}$. Evaluating this dot product using the relations in (3.6) is easy. Using (3.5) we have

$$\begin{aligned}\text{Fig. 1(a):}\quad D^{-1}\cdot D^{-1}&=a^{-d-2}[\underline{(1)}-2d\underline{(0)}]\cdot a^{-d-2}[\underline{(1)}-2d\underline{(0)}]\\&=a^{-2d-4}[\underline{(1)}\cdot\underline{(1)}-4d\underline{(0)}\cdot\underline{(1)}+4d^2\underline{(0)}\cdot\underline{(0)}]\\&=a^{-2d-4}[\underline{(1)}+4d^2\underline{(0)}].\end{aligned} \tag{3.7}$$

Evaluating the graphs in Fig. 1(b) and 1(c) is just as easy:

$$\text{Fig. 1(b):}\quad D^{-1}\cdot D^{-1}\cdot D^{-1}=a^{-3d-6}[\underline{(1)}-8d^3\underline{(0)}], \tag{3.8}$$

$$\text{Fig. 1(c):}\quad D^{-1}\cdot D^{-1}\cdot D^{-1}\cdot D^{-1}=a^{-4d-8}[\underline{(1)}+16d^4\underline{(0)}]. \tag{3.9}$$

Series structures in propagator graphs—convolution products

A slightly more complicated graphical structure is a series structure. For example, in Fig. 2(a) we have two lines D^{-1} in series. We represent such a structure using the notation $D^{-1}\times D^{-1}$. To evaluate such a propagator graph in one dimension we must perform a sum over the position of the intermediate vertex:

$$\begin{aligned}a^{-3}(1\ -2\ 1)\times a^{-3}(1\ -2\ 1)&=a\sum_j a^{-3}(\delta_{i,j+1}-2\delta_{i,j}+\delta_{i+1,j})a^{-3}(\delta_{j,k+1}-2\delta_{j,k}+\delta_{j+1,k})\\&=a^{-5}(\delta_{i,k+2}-4\delta_{i,k+1}+6\delta_{i,k}-4\delta_{i+1,k}+\delta_{i+2,k})=a^{-5}(1\ -4\ 6\ -4\ 1).\end{aligned} \tag{3.10a}$$

An evaluation of $D^{-1}\times D^{-1}$ by a similar procedure in 2 dimensions gives the matrix

$$a^{-6}\begin{bmatrix} & & 1 & & \\ & 2 & -8 & 2 & \\ 1 & -8 & 20 & -8 & 1 \\ & 2 & -8 & 2 & \\ & & 1 & & \end{bmatrix}. \tag{3.10b}$$

It is obviously rather messy to perform such a sum on a d-dimensional lattice. However, it is easy to compute graphs like $D^{-1}\times D^{-1}$ using the following convolution rules:

$$\underline{(0)}\times(\text{any}) = (\text{any}), \tag{3.11a}$$

$$\underline{(1)}\times\underline{(1)} = 2d\underline{(0)} + \underline{(2)} + 2\underline{(11)}, \tag{3.11b}$$

$$\underline{(1)}\times\underline{(2)} = \underline{(1)} + \underline{(3)} + \underline{(12)}, \tag{3.11c}$$

$$\underline{(2)}\times\underline{(2)} = 2d\underline{(0)} + 2\underline{(22)} + \underline{(4)}, \tag{3.11d}$$

$$\underline{(1)}\times\underline{(11)} = 2(d-1)\underline{(1)} + \underline{(12)} + 3\underline{(111)}. \tag{3.11e}$$

[It is fairly easy to derive (3.11) using elementary combinatoric arguments.]

Using (3.11) we evaluate $D^{-1}\times D^{-1}$ as follows:

$$a^d a^{-d-2}[\underline{(1)} - 2d\underline{(0)}]\times a^{-d-2}[\underline{(1)} - 2d\underline{(0)}] = a^{-d-4}[\underline{(1)}\times\underline{(1)} - 4d\underline{(0)}\times\underline{(1)} + 4d^2\underline{(0)}\times\underline{(0)}]$$

$$= a^{-d-4}[(2d + 4d^2)\underline{(0)} - 4d\underline{(1)} + \underline{(2)} + 2\underline{(11)}]. \tag{3.12}$$

Note that the symbol $\times$ implies that an integration (sum) is being performed so it is associated with a factor of a^d.

Now let us evaluate some other convolution graphs using the algebraic rules in (3.11).

Fig. 2(b): $$D^{-1}\times(D^{-1}\cdot D^{-1}) = a^{-2d-6}[(2d - 8d^3)\underline{(0)} + \underline{(2)} + 2\underline{(11)} + (4d^2 - 2d)\underline{(1)}], \tag{3.13}$$

Fig. 2(c): $$(D^{-1}\cdot D^{-1})\times(D^{-1}\cdot D^{-1}) = a^{-3d-8}[(2d + 16d^4)\underline{(0)} + 8d^2\underline{(1)} + \underline{(2)} + 2\underline{(11)}], \tag{3.14}$$

Fig. 2(d): $$D^{-1}\times D^{-1}\times D^{-1} = a^{-d-6}[(-12d^2 - 8d^3)\underline{(0)} + (12d^2 + 6d - 3)\underline{(1)} - 6d\underline{(2)} - 12d\underline{(11)} + \underline{(3)} + 3\underline{(12)} + 6\underline{(111)}]. \tag{3.15}$$

Combined series and parallel structures in propagator graphs

Almost all propagator graphs are a combination of series and parallel structures and are therefore easy to evaluate using the algebraic rules in (3.6) and (3.11). Five typical graphs are indicated in Fig. 3. We evaluate these graphs below.

Fig. 3(a): $$(D^{-1}\times D^{-1}\times D^{-1})\cdot D^{-1} = a^{-2d-8}[(24d^3 + 16d^4)\underline{(0)} + (12d^2 + 6d - 3)\underline{(1)}], \tag{3.16}$$

Fig. 3(b): $$(D^{-1}\times D^{-1})\cdot(D^{-1}\times D^{-1}\times D^{-1}) = a^{-2d-10}[(-24d^3 - 64d^4 - 32d^5)\underline{(0)} + (-48d^3 - 24d^2 + 12d)\underline{(1)} - 6d\underline{(2)} - 24d\underline{(11)}], \tag{3.17}$$

Fig. 3(c): $$(D^{-1}\times D^{-1}\times D^{-1})\cdot(D^{-1}\times D^{-1})\cdot D^{-1} = a^{-3d-12}[(64d^6 + 128d^5 + 48d^4)\underline{(0)} + (-48d^3 - 24d^2 + 12d)\underline{(1)}], \tag{3.18}$$

Fig. 3(d): $$[D^{-1}\times(D^{-1}\cdot D^{-1}\cdot D^{-1})]\cdot D^{-1} = a^{-4d-10}[(-4d^2 - 32d^5)\underline{(0)} + (-2d - 8d^3)\underline{(1)}], \tag{3.19}$$

Fig. 3(e): $$[(D^{-1}\cdot D^{-1})\times(D^{-1}\cdot D^{-1})]\cdot D^{-1} = a^{-4d-10}[(-4d^2 - 32d^5)\underline{(0)} + 8d^2\underline{(1)}]. \tag{3.20}$$

Reduction of propagator graphs to vacuum graphs

Vacuum graphs (graphs having no external legs) are numbers (rather than matrices) which depend on the dimension d of the lattice. As we will see in Sec. IV, the vacuum graphs are the basic building blocks of the coefficients of the effective potential. There are two simple methods for obtaining vacuum graphs from propagator graphs.

Method 1. We can attach the two ends of a propagator graph together. In the continuum this consists of taking a propagator function in coordinate space, say $P(x,y)$, and attaching the points x and y using a δ function:

$$\int dx\,\delta(x-y)P(x,y).$$

On the lattice we do the equivalent thing. A δ function on the lattice is just

$$\delta(x-y) \to a^{-d}\underline{(0)}. \tag{3.21}$$

We must dot the lattice propagator graph with $a^{-d}\underline{(0)}$, which just projects out the $\underline{(0)}$ part of the graph, and then we integrate over all space (sum over all lattice points) using the formula

$$a^d \sum_{\substack{\text{lattice}\\ \text{points}}} a^{-d}\underline{(0)} = 1. \tag{3.22}$$

The final result is this. *Attaching the ends of a propagator graph generates a vacuum graph whose value is the coefficient of the* $(\underline{0})$ *term in the propagator graph.* Here are several examples.

Fig. 4(a): The coefficient of $(\underline{0})$ in $D^{-1}\times D^{-1}$ is $a^{-d-4}(2d+4d^2)$. (3.23)

Fig. 4(b): The coefficient of $(\underline{0})$ in $D^{-1}\cdot D^{-1}$ is $a^{-2d-4}4d^2$. (3.24)

Fig. 4(c): The coefficient of $(\underline{0})$ in $(D^{-1}\cdot D^{-1})\times(D^{-1}\cdot D^{-1})$ is $a^{-3d-8}(2d+16d^4)$. (3.25)

Fig. 4(d): The coefficient of $(\underline{0})$ in $(D^{-1}\times D^{-1}\times D^{-1})$ is $a^{-d-6}(-12d^2-8d^3)$. (3.26)

Fig. 4(e): The coefficient of $(\underline{0})$ in $[(D^{-1}\times D^{-1}\times D^{-1})\cdot D^{-1}]\times(D^{-1}\cdot D^{-1})$ is $a^{3d-12}(64d^6+96d^5+24d^3+12d^2-6d)$. (3.27)

Method 2. A propagator graph in coordinate space is translation invariant,

$$P(x,y)=P(x-y).$$

Therefore, integrating $P(x,y)$ over all x produces a constant, and this constant is the numerical value of the vacuum graph obtained by removing the legs from the propagator graph. The equivalent operation on the lattice is obtained by summing over all lattice points using the formulas

$$\begin{aligned}
&\sum(\underline{0})=1,\\
&\sum(\underline{1})=2d,\\
&\sum(\underline{2})=2d,\\
&\sum(\underline{3})=2d,\\
&\sum(\underline{11})=2d(d-1),\\
&\sum(\underline{111})=\tfrac{4}{3}d(d-1)(d-2),\\
&\sum(\underline{12})=4d(d-1).
\end{aligned} \tag{3.28}$$

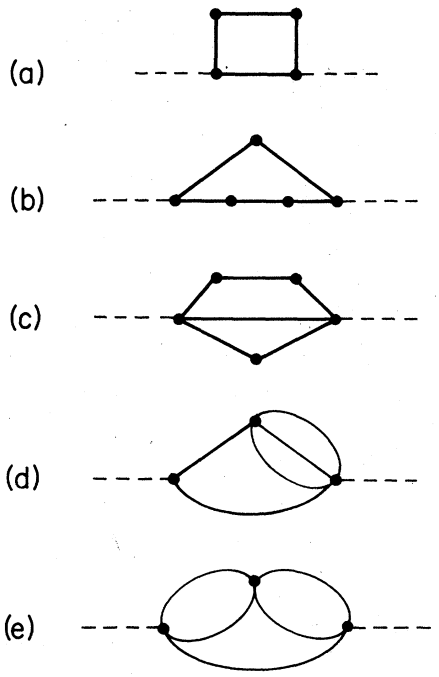

FIG. 3. Propagator graphs with combined series and parallel structure.

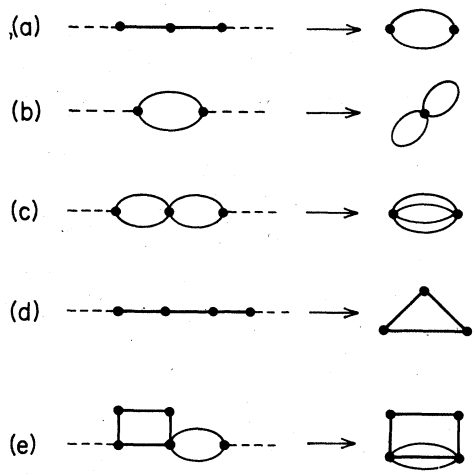

FIG. 4. Creating vacuum graphs from propagator graphs by attaching the two ends of the propagator together.

When performing the sum over all lattice points to obtain the vacuum graph it is necessary to multiply by a^d because the sum is really equivalent to an integral. Here are several examples taken from Fig. 5:

Fig. 5(a): $a^d \sum D^{-1} \cdot D^{-1} = a^{-d-4} \sum [4d^2(\underline{0}) + (\underline{1})] = a^{-d-4}(4d^2 + 2d)$,

which agrees with the result in (3.23);

Fig. 5(b): $a^d \sum [D^{-1} \times D^{-1}] \cdot D^{-1} = a^{-d-6} \sum [-(4d^2 + 8d^3)(\underline{0}) - 4d(\underline{1})] = a^{-d-6}[-12d^2 - 8d^3]$,

which agrees with the result in (3.26);

Fig. 5(c): $a^d \sum D^{-1} \times D^{-1} \times D^{-1} = 0$; (3.29)

Fig. 5(d): $a^d \sum (D^{-1} \times D^{-1} \times D^{-1}) \cdot (D^{-1} \times D^{-1} \times D^{-1}) = a^{-3d-12}(64d^6 + 480d^5 + 720d^4 - 240d^3 - 180d^2 + 80d)$. (3.30)

Properties of vacuum graphs

The result in (3.29) is a specific case of a general property of vacuum graphs; namely, that there are no nonvanishing one-particle-reducible (tadpole) vacuum graphs.

To help in the computation of vacuum graphs it is useful to know that vacuum graphs which are one-vertex reducible can be expressed as the product of the two simpler vacuum graphs obtained by cutting the reducible vacuum graph at a vertex. (This property is illustrated in Fig. 6.) Thus, any vacuum graph can be expressed as a product of one-vertex-irreducible subgraphs (OVIS's). All vacuum OVIS's having from one through six lines are shown in Fig. 7.

The OVIS's in Fig. 7 illustrate a general property of vacuum graphs. Every vacuum graph having n D^{-1} lines is a *polynomial* in the variable $(-2d)$ of degree n which vanishes at $d = 0$. The coefficient of the $(-2d)^n$ term is one. Once the vacuum graphs have been expressed as polynomials in the dimension d, there is no need for d to be an integer. Indeed, the polynomials are a simple analytic continuation of the graphs of the theory to arbitrary complex dimension d. Had these calculations been performed on a hyper-body-centered cubic lattice the result would have been a sum of exponentials of d.[7]

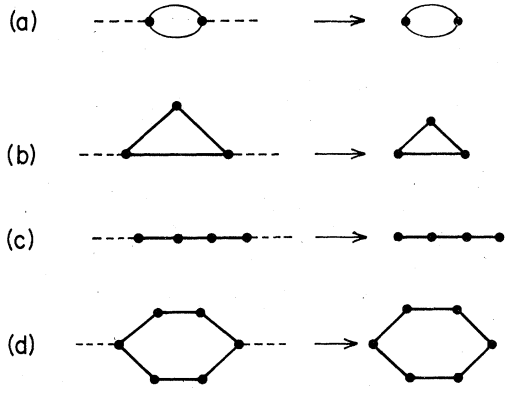

FIG. 5. Creating vacuum graphs from propagator graphs by integrating over the position of one external vertex.

Graphs having more than parallel and series components

All but one of the OVIS's shown in Fig. 7 can be evaluated in seconds using the parallel and series algebraic rules for propagators and the two methods for reducing propagator graphs to vacuum graphs. However, the tetrahedron or cross-box graph shown last in Fig. 7 cannot be computed using the algebraic rules we have given so far. This is because it is not a simple combination of parallel and series structures.

To evaluate the vacuum tetrahedron graph we consider the propagator graph shown in Fig. 8(a). This graph is a parallel structure formed by combining D^{-1} with the simpler propagator in Fig. 8(b). This propagator is in turn formed by combining the two *three*-legged graphs shown in Fig. 8(c) and Fig. 8(d). Apparently, it is necessary to know how to represent a three-legged graph before we can proceed. We will see that a three-legged graph is a matrix whose elements are *matrices* rather than numbers as was the case with two-legged propagator graphs. (Four-legged graphs are matrices of matrices of matrices, and so on.)

We examine the problem first on a one-dimensional lattice. To begin, we represent the graph in Fig. 8(c) as a matrix of matrices,

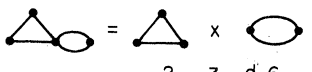

$= (-12d^2 - 8d^3)a^{-d-6} \times (2d + 4d^2)a^{-d-4}$

$= (-32d^5 - 64d^4 - 24d^3)a^{-2d-10}$

FIG. 6. A one-vertex-reducible graph expressed as the product of its two irreducible OVIS's.

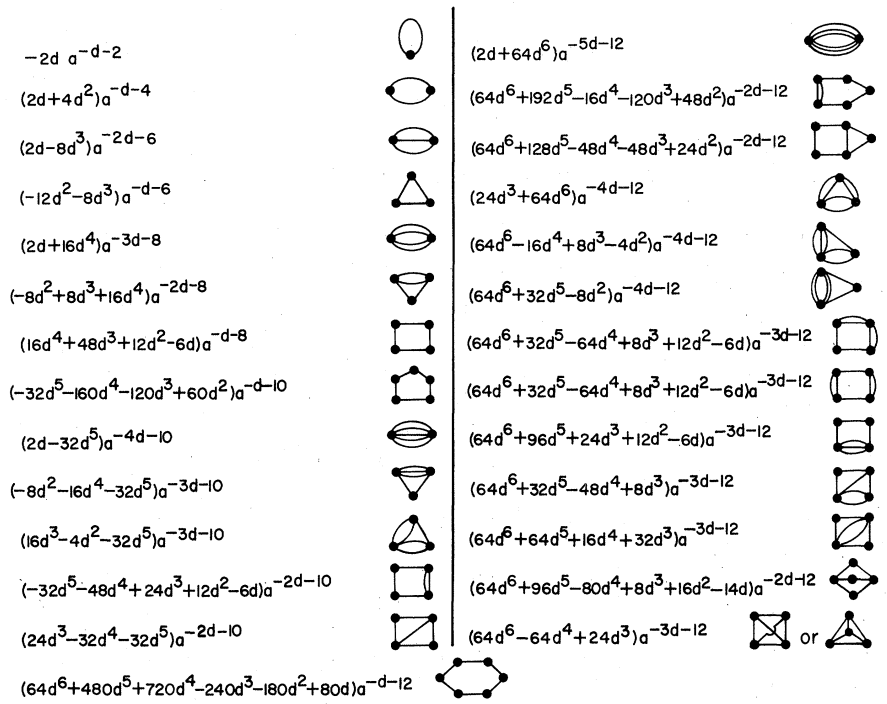

FIG. 7. All one-vertex-irreducible vacuum graphs having from one through six internal lines. Along side each OVIS is its numerical value. The OVIS's are the basic building blocks of all vacuum graphs; any vacuum graph can be expressed as a product of its OVIS's as in Fig. 6.

$$a^{-6}\left[\begin{pmatrix}1\\0\\0\end{pmatrix},\begin{pmatrix}-2\\-2\\0\end{pmatrix},\begin{pmatrix}1\\4\\1\end{pmatrix},\begin{pmatrix}0\\-2\\-2\end{pmatrix},\begin{pmatrix}0\\0\\1\end{pmatrix}\right]. \tag{3.31}$$

This expression is obtained by a new algebraic operation. The structure in (3.31) is an *outer* product of the D^{-1} matrix $a^{-3}(1,-2,1)$ with itself: Working from left to right, the first nonzero element is 1×1, the next two are $1\times(-2)$ and $(-2)\times 1$, the next three are 1×1, $(-2)\times(-2)$, and 1×1, the next two are $(-2)\times 1$ and $1\times(-2)$, and the last is 1×1. This makes a total of nine nonzero elements—all the combinations of $(1,-2,1)$ with itself. Observe that the matrix in (3.31) has five horizontal elements [this represents a two-lattice-unit propagation from the left-hand side to the right-hand side of Fig. 8(c), just as in (3.10a)] and three vertical elements [this represents a one-lattice-unit propagation from the left- (or right-) hand side of the graph to the center of the graph].

Next, we construct the graph in Fig. 8(d) by making a series connection to D^{-1} at the center of the graph in Fig. 8(c). The result is

$$a^{-8}\left[\begin{pmatrix}1\\-2\\1\\0\\0\end{pmatrix},\begin{pmatrix}-2\\2\\2\\-2\\0\end{pmatrix},\begin{pmatrix}1\\2\\-6\\2\\1\end{pmatrix},\begin{pmatrix}0\\-2\\2\\2\\-2\end{pmatrix},\begin{pmatrix}0\\0\\1\\-2\\1\end{pmatrix}\right]. \tag{3.32}$$

This expression is obtained by taking five separate cross products

$$(1\ 0\ 0)\times(1\ -2\ 1)=(1\ -2\ 1\ 0\ 0),$$
$$(-2\ -2\ 0)\times(1\ -2\ 1)=(-2\ 2\ 2\ -2\ 0),$$
$$(1\ 4\ 1)\times(1\ -2\ 1)=(1\ 2\ -6\ 2\ 1),$$
$$(0\ -2\ -2)\times(1\ -2\ 1)=(0\ -2\ 2\ 2\ -2),$$
$$(0\ 0\ 1)\times(1\ -2\ 1)=(0\ 0\ 1\ -2\ 1).$$

Next, we construct the propagator graph in Fig. 8(b) by dotting together and integrating (method 2)

the expression in (3.31) and (3.32):

$$a^{-13}[-2,-8,-20,-8,2]=a^{-13}[-2(\underline{2})\ -8(\underline{1})\ -20(\underline{0})]\,. \tag{3.33}$$

Here we have used the product relations

$$\sum(1\ 0\ 0)\cdot(1\ -2\ 1\ 0\ 0)=\sum(-2\ 0\ 0)=-2\,,$$

$$\sum(-2\ -2\ 0)\cdot(-2\ 2\ 2\ -2\ 0)=\sum(-4\ -4\ 0)=-8\,,$$

$$\sum(1\ 4\ 1)\cdot(1\ 2\ -6\ 2\ 1)=\sum(2\ -24\ 2)=-20\,.$$

Finally, we dot the result in (3.33) with D^{-1}, $a^{-3}(1\ -2\ 1)$, to obtain the cross-box propagator graph in Fig. 8(a):

$$a^{-16}[-8\ 40\ -8]=a^{-16}[40(\underline{0})-8(\underline{1})] \tag{3.34}$$

and we use method 2 to evaluate the tetrahedron vacuum graph in one dimension:

$$a\sum a^{-16}[40(\underline{0})-8(\underline{1})]=a^{-15}(40-16)=24a^{-15}\,. \tag{3.35}$$

It is slightly more difficult to repeat the above calculation on a two-dimensional lattice. The analog of (3.31) is

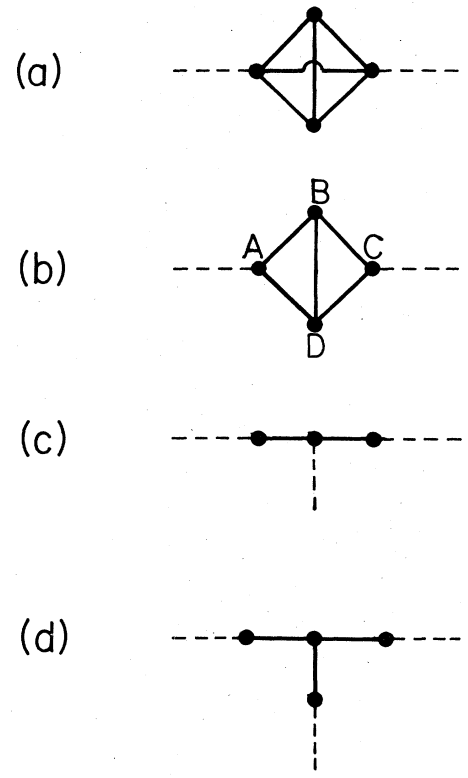

FIG. 8. Evaluation of the cross-box propagator. The calculation begins with finding the three-legged graphs in (c) and (d) and dotting them together to produce the propagator in (b). This graph is dotted with G^{-1} to produce the cross-box propagator in (a).

$$a^{-8}\begin{bmatrix} & & & \begin{pmatrix}1\\0\ 0\ 0\\0\end{pmatrix} & \\ & \begin{pmatrix}1\\1\ 0\ 0\\0\end{pmatrix} & \begin{pmatrix}-4\\0\ -4\ 0\\0\end{pmatrix} & \begin{pmatrix}1\\0\ 0\ 1\\0\end{pmatrix} & \\ \begin{pmatrix}0\\1\ 0\ 0\\0\end{pmatrix} & \begin{pmatrix}0\\-4\ -4\ 0\\0\end{pmatrix} & \begin{pmatrix}1\\1\ 16\ 1\\1\end{pmatrix} & \begin{pmatrix}0\\0\ -4\ -4\\0\end{pmatrix} & \begin{pmatrix}0\\0\ 0\ 1\\0\end{pmatrix} \\ & \begin{pmatrix}0\\1\ 0\ 0\\1\end{pmatrix} & \begin{pmatrix}0\\0\ -4\ 0\\-4\end{pmatrix} & \begin{pmatrix}0\\0\ 0\ 1\\1\end{pmatrix} & \\ & & \begin{pmatrix}0\\0\ 0\ 0\\1\end{pmatrix} & & \end{bmatrix} \tag{3.36}$$

and the analog of (3.32) is

$$a^{-10}\begin{bmatrix}
\begin{pmatrix} & 0 & \\ 1 & 0 & 0 \\ 1 & -4 & 1 & 0 & 0 \\ 1 & 0 & 0 \\ & 0 & \end{pmatrix}
\begin{pmatrix} & 0 & \\ -4 & -4 & 0 \\ -4 & 12 & 12 & -4 & 0 \\ -4 & -4 & 0 \\ & 0 & \end{pmatrix}
\begin{pmatrix} & 1 & \\ 2 & 12 & 2 \\ 1 & 12 & -60 & 12 & 1 \\ 2 & 12 & 2 \\ & 1 & \end{pmatrix}
\begin{pmatrix} & 0 & \\ 0 & -4 & -4 \\ 0 & -4 & 12 & 12 & -4 \\ 0 & -4 & -4 \\ & 0 & \end{pmatrix}
\begin{pmatrix} & 0 & \\ 0 & 0 & 1 \\ 0 & 0 & 1 & -4 & 1 \\ 0 & 0 & 1 \\ & 0 & \end{pmatrix} \\
\begin{pmatrix} & 1 & \\ 2 & -4 & 1 \\ 1 & -4 & 2 & 0 & 0 \\ 1 & 0 & 0 \\ & 0 & \end{pmatrix}
\begin{pmatrix} & -4 & \\ -4 & 12 & -4 \\ 0 & -4 & 12 & -4 & 0 \\ 0 & -4 & 0 \\ & 0 & \end{pmatrix}
\begin{pmatrix} & 1 & \\ 1 & -4 & 2 \\ 0 & 0 & 2 & -4 & 1 \\ 0 & 0 & 1 \\ & 0 & \end{pmatrix}
\begin{pmatrix} & 0 & \\ 1 & 0 & 0 \\ 1 & -4 & 2 & 0 & 0 \\ 2 & -4 & 1 \\ & 1 & \end{pmatrix}
\begin{pmatrix} & 0 & \\ 0 & -4 & 0 \\ 0 & -4 & 12 & -4 & 0 \\ -4 & 12 & -4 \\ & -4 & \end{pmatrix}
\begin{pmatrix} & 0 & \\ 0 & 0 & 1 \\ 0 & 0 & 2 & -4 & 1 \\ 1 & -4 & 2 \\ & 1 & \end{pmatrix} \\
\begin{pmatrix} & 0 & \\ 0 & 0 & 0 \\ 0 & 0 & 1 & 0 & 0 \\ 1 & -4 & 1 \\ & 1 & \end{pmatrix}
\begin{pmatrix} & 1 & \\ 1 & -4 & 1 \\ 0 & 0 & 1 & 0 & 0 \\ 0 & 0 & 0 \\ & 0 & \end{pmatrix}
\end{bmatrix}.$$

Dotting and summing (3.36) and (3.37) gives the analog of (3.33),

$$a^{-16}\begin{pmatrix} & -4 & \\ -8 & -96 & -8 \\ -4 & -96 & -912 & -96 & -4 \\ -8 & -96 & -8 \\ & -4 & \end{pmatrix} = a^{-16}[-4(\underline{2}) - 8(\underline{11}) - 96(\underline{1}) - 912(\underline{0})].$$

Hence the two-dimensional cross-box propagator in Fig. 8(a) is

$$a^{-20}\begin{pmatrix} & -96 & \\ -96 & 3648 & -96 \\ & -96 & \end{pmatrix} = a^{-20}[3648(\underline{0}) - 96(\underline{1})] \tag{3.37}$$

and the value of the two-dimensional tetrahedron vacuum graph is

$$3264a^{-18}. \tag{3.38}$$

The generalization of these calculations to d dimensions is described below. The answers are as follows: The propagator graph in Fig. 8(b) is

$$a^{-3d-10}[(-32d^5+16d^3-4d^2)(\underline{0}) + (8d^2-16d^3)(\underline{1}) - 2d(\underline{2}) - 4d(\underline{11})], \tag{3.39}$$

the cross-box propagator graph in Fig. 8(a) is

$$a^{-4d-12}(64d^6-32d^4+8d^3)(\underline{0}) + (8d^2-16d^3)(\underline{1}), \tag{3.40}$$

and the value of the tetrahedron vacuum graph is

$$a^{-3d-12}[64d^6-64d^4+24d^3]. \tag{3.41}$$

To derive the result in (3.39) refer to Fig. 8(b). Since the shortest path from A to C has length 2,

it follows that the propagator in Fig. 8(b) has the form

$$\alpha\underline{0}+\beta\underline{1}+\gamma\underline{11}+\delta\underline{2}\,,$$

where α, β, γ, δ are d-dependent constants.

The coefficient δ is trivially obtained. Locate A at the origin and C at $(2,0,0\ldots)$. Then the only nonzero contribution to the graph comes when both B and D are at $(1,0,0\ldots)$. Then each of the lines AB, AD, BC, CD contribute a factor 1, while BD contributes $-2d$. Hence,

$$\delta=-2d\,.$$

To find γ, set C at $(1,1,0,0\ldots)$. Then B can be at $(1,0,0\ldots)$ or at $(0,1,\ldots,0)$. Similarly for D. But since B and D are connected, at most one of their coordinate components can differ. In this case, they must be at the same point. So

$$\gamma=2(-2d)\,,$$

where the first factor of 2 comes from the two possible locations of B.

To find β, set C at $(1,0,0\ldots)$. Then B can either be at the origin or at C, and similarly for D. So

$$\beta=(-2d)^3+(-2d)^2+(-2d)^2+(-2d)^3$$
$$=-16d^3+8d^2\,.$$

Finally, to find α set C at the origin. Then B can be either at the origin or at one of the $2d$ nearest neighbors of the origin. Similarly for D. But since B and D are connected, if neither is at the origin, they must both be at the same point. When both B and D are at the origin, the contribution to α is

$$(-2d)^5\,.$$

When B is at the origin and D at one of the $2d$ nearest neighbors, the contribution to α is

$$(2d)(-2d)^2=8d^3\,,$$

and similarly when D is at the origin and B is not. Finally, when B and D are both not at the origin, the contribution to α is

$$(2d)(-2d)=-4d^2\,.$$

Thus,

$$\alpha=-32d^5+16d^3-4d^2\,.$$

Evaluation of two difficult seven-line propagator graphs

Two difficult-to-evaluate seven-line propagator graphs are shown in Figs. 9(a) and 9(e). We review the ideas presented in the last subsection by computing these graphs.

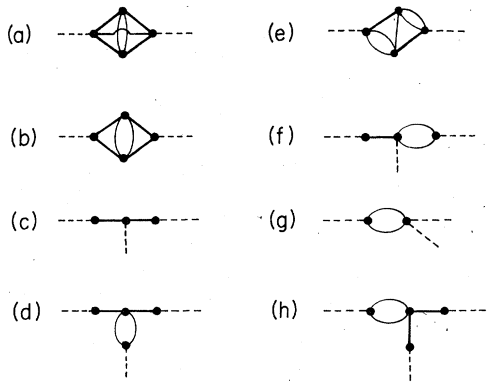

FIG. 9. Two difficult-to-evaluate seven-line propagator graphs are shown in (a) and (e). To construct (a) the two three-point graphs in (c) and (d) are dotted together to produce (b), which is in turn dotted with G^{-1}. To construct (e) the two three-point graphs in (f) and (h) are dotted together.

First, we compute the graph in Fig. 9(a) on a one-dimensional lattice. We begin with the three-legged graph in Fig. 9(c) which is given in (3.31) and cross this graph in the vertical direction with $D^{-1}\cdot D^{-1}=a^{-6}(1\ 4\ 1)$ to produce the three-legged graph in Fig. 9(d):

$$a^{-11}\left[\begin{pmatrix}1\\4\\1\\0\\0\end{pmatrix},\begin{pmatrix}-2\\-10\\-10\\-2\\0\end{pmatrix},\begin{pmatrix}1\\8\\18\\8\\1\end{pmatrix},\begin{pmatrix}0\\-2\\-10\\-10\\-2\end{pmatrix},\begin{pmatrix}0\\0\\1\\4\\1\end{pmatrix}\right] \tag{3.42}$$

Next, (3.31) and (3.42) are dotted and summed to give the propagator graph in Fig. 9(b):

$$a^{-16}[4\ 40\ 88\ 40\ 4]=a^{-16}[4(\underline{2})+40(\underline{1})+88(\underline{0})]\,. \tag{3.43}$$

Finally, we dot (3.43) with $D^{-1}=a^{-3}(1\ -2\ 1)$ to produce the propagator graph in Fig. 9(a):

$$a^{-19}(40\ -176\ 40)=a^{-19}[40(\underline{1})-176(\underline{0})]\,. \tag{3.44}$$

Repeating this procedure in d dimensions gives

$$a^{-4d-12}[(24d^3+64d^6)(\underline{0})+(8d^2+32d^4)(\underline{1})$$
$$+4d^2(\underline{2})+8d^2(\underline{11})] \tag{3.45}$$

for the propagator in Fig. 9(b) and

$$a^{-5d-14}[(-48d^4-128d^7)(\underline{0})+(8d^2+32d^4)(\underline{1})] \tag{3.46}$$

for the propagator in Fig. 9(a).

Now consider the graph in Fig. 9(e). Again we examine the one-dimensional case first. In one dimension, the graph in Fig. 9(f) is

$$a^{-9}\left[\begin{pmatrix}1\\0\\0\end{pmatrix},\begin{pmatrix}4\\-2\\0\end{pmatrix},\begin{pmatrix}1\\-8\\1\end{pmatrix},\begin{pmatrix}0\\-2\\4\end{pmatrix},\begin{pmatrix}0\\0\\1\end{pmatrix}\right] \tag{3.47}$$

and the graph in Fig. 9(g) is

$$a^{-9}\left[\begin{pmatrix}1\\0\\0\end{pmatrix},\begin{pmatrix}-2\\4\\0\end{pmatrix},\begin{pmatrix}1\\-8\\1\end{pmatrix},\begin{pmatrix}0\\4\\-2\end{pmatrix},\begin{pmatrix}0\\0\\1\end{pmatrix}\right]. \tag{3.48}$$

Crossing (3.48) with D^{-1} in the vertical direction gives Fig. 9(h),

$$a^{-11}\left[\begin{pmatrix}1\\-2\\1\\0\\0\end{pmatrix},\begin{pmatrix}-2\\8\\-10\\4\\0\end{pmatrix},\begin{pmatrix}1\\-10\\18\\-10\\1\end{pmatrix},\begin{pmatrix}0\\4\\-10\\8\\-2\end{pmatrix},\begin{pmatrix}0\\0\\1\\-2\\1\end{pmatrix}\right]. \tag{3.49}$$

We obtain the desired propagator graph in Fig. 9(e) by dotting and summing (3.48) and (3.49):

$$a^{-19}(-2,52,-164,52,-2)=a^{-17}[-2(\underline{2})+52(\underline{1})-164(\underline{0})]. \tag{3.50}$$

The same procedure in d dimensions gives

$$a^{-5d-14}[(-4d^2-32d^4-128d^7)(\underline{0})+(48d^4+4d^2)(\underline{1})-2d(\underline{2})-4d(\underline{11})], \tag{3.51}$$

for the propagator graph in Fig. 9(e).

Fourier-transforming propagator graphs to momentum space

It is necessary to transform propagator graphs for the two-point function to momentum space to determine the wave-function renormalization constant and the locations of the poles. We first describe this procedure in one-dimensional space where we need not consider the problem of lack of rotational invariance.

Let p^2 be the Euclidean momentum squared and p_M^2 be the Minkowski momentum squared. Then the Fourier transform of $D^{-1}=\partial^2\delta(x-y)$ is simply $-p^2=p_M^2$.[8] The Fourier transform of series iterated factors of D^{-1} is also simple: The Fourier transform of the convolution $D^{-1}\times D^{-1}\times\cdots\times D^{-1}$ (n factors) is $(-p^2)^n=p_M^{2n}$. The strategy is clearly to reexpress a propagator graph which was originally computed as a linear combination of the basis vectors $(\underline{0})$, $(\underline{1})$, $(\underline{2})$, (3),... in terms of the basis vectors $\delta(x-y)$, D^{-1}, $D^{-1}\times D^{-1}$, $D^{-1}\times D^{-1}\times D^{-1}$, ... :

$$\begin{aligned}
(\underline{0}) &= a\delta(x-y)\,,\\
(\underline{1}) &= a^3D^{-1}(x-y)+2a\delta(x-y)\,,\\
(\underline{2}) &= a^5D^{-1}\times D^{-1}+4a^3D^{-1}+2a\delta(x-y)\,,\\
(\underline{3}) &= a^7D^{-1}\times D^{-1}\times D^{-1}+6a^5D^{-1}\times D^{-1}\\
&\quad +9a^3D^{-1}+2a\delta(x-y)
\end{aligned}$$

and so on. Now if we take the Fourier transform, we find that

$$\begin{aligned}
\mathcal{F}(\underline{0}) &= a\,,\\
\mathcal{F}(\underline{1}) &= a^3p_M^2+2a\,,\\
\mathcal{F}(\underline{2}) &= a^5p_M^4+4a^3p_M^2+2a\,,\\
\mathcal{F}(\underline{3}) &= a^7p_M^6+6a^5p_M^4+9a^3p_M^2+2a
\end{aligned} \tag{3.52}$$

and so on.

Here are three examples. From (3.9) the Fourier transform of the graph in Fig. 1(c) is $a^{-9}p_M^2+18a^{-11}$. From (3.14) the Fourier transform of the graph in Fig. 2(c) is $a^{-6}p_M^4+12a^{-8}p_M^2+36a^{-10}$. From (3.43) the Fourier transform of the graph in Fig. 9(b) is $4a^{-11}p_M^4+56a^{-13}p_M^2+126a$.

The one remaining question is how to perform Fourier transforms when $d>1$ and the lattice is not rotationally invariant. We handle this problem as follows. Since the continuum *is* rotationally invariant we expect the continuum answer to depend only on the variable p_M^2. However, the method we have been using to take Fourier transforms will give nonrotationally invariant expressions like $\sum_{i=1}^{d}(p_M)_i^4$, where $(p_M)_i$ is the ith component of the momentum vector p_M. We therefore perform a Lorentz transformation so that the momentum vector p_M points along the 1 axis and its compon-

ents in the other directions all vanish. Now we cannot distinguish $\sum_{i=1}^{d}(p_M)_i^4$ from the rotationally invariant expression $[\sum_{i=1}^{d}(p_M)_i^2]^2 = p_M^4$. Any errors incurred by rotationally symmetrizing momentum dependent expressions in the manner just described vanish with the lattice spacing. From this argument we conclude that we can replace the Fourier transform of $6d(\underline{0}) - 4(\underline{1}) + (\underline{2})$, which is $a^{d+4}\sum_{i=1}^{d}(p_M)_i^4$, by $a^{d+4}p_M^4$.

We thus obtain the d-dimensional generalization of the Fourier transform relations in (3.52):

$$\begin{aligned}
&\mathfrak{F}(\underline{0}) = a^d\,,\\
&\mathfrak{F}(\underline{1}) = 2da^d + p_M^2 a^{2+d}\,,\\
&\mathfrak{F}(\underline{2}) = 2da^d + 4p_M^2 a^{2+d} + p_M^4 a^{4+d}\,,\\
&\mathfrak{F}(\underline{11}) = (2d^2 - 2d)a^d + p_M^2(2d-2)a^{2+d}\,.
\end{aligned} \tag{3.53}$$

Using (3.52) we generalize to d-dimensional lattices the three previous examples of one-dimensional Fourier transforms. From (3.9) the Fourier transform of the graph in Fig. 1(c) is $(2d+16d^2)a^{-3d-8} + p_M^2 a^{-3d-6}$. From (3.14) the Fourier transform of the graph in Fig. 2(c) is $(16d^4+16d^3+4d^2)\,a^{-2d-8} + (8d^2+4d)p_M^2 a^{-2d-6} + p_M^4 a^{-2d-4}$. From (3.45) the Fourier transform of the graph in Fig. 9(b) is $a^{-12-3d}(64d^6+64d^5+16d^4+32d^3) + a^{-10-3d} \times p_M^2(32d^4+8d^2+16d^3) + a^{-8-3d}p_M^4(4d^2)$.

Note that the d-dimensional Fourier transform of a propagator graph in d dimensions is always a polynomial in p_M^2 where the degree of the polynomial is the smallest number of lattice units linking one external vertex to the other.

IV. CALCULATION OF THE EFFECTIVE POTENTIAL

In Secs. II and III we determined the strong-coupling expansions for the vertices and gave a general prescription for evaluating diagrams having zero and two external legs. As we will show, these techniques are sufficient to compute the effective potential. Specifically, we will see that the fundamental constituents of all of the coefficients of the effective potential are the vacuum OVIS's discussed in Sec. III.[9]

One-particle irreducibility

To prepare for our discussion of the effective potential we must introduce the notation of a one-particle irreducible graph. This is a graph which does not separate into two graphs when one internal line is cut. In Fig. 10(a) we give two examples of one-particle-reducible graphs and in Fig. 10(b) we give two examples of one-particle-irreducible graphs. It is important to remark that one-particle irreducibility is a topological property of a graph. The lines in the graph can represent different objects depending on the expansion being used: In strong-coupling expansions the lines represent $D^{-1}(x,y)$, in weak-coupling expansions the lines represent $[D^{-1}(x,y) + m^2\delta(x-y)]^{-1}$, and when expressing the full n-point Green's functions of the theory in terms of the full one-particle irreducible vertices Γ_n, the lines represent the full propagators W_2 (see Fig. 12). One of the goals of this section is to show that if we define Λ_{2n} as the sum of all one-particle-irreducible strong-coupling diagrams having $2n$ external legs, then all of the coefficients V_{2n} of the effective potential can be expressed simply in terms of Λ_{2n}.

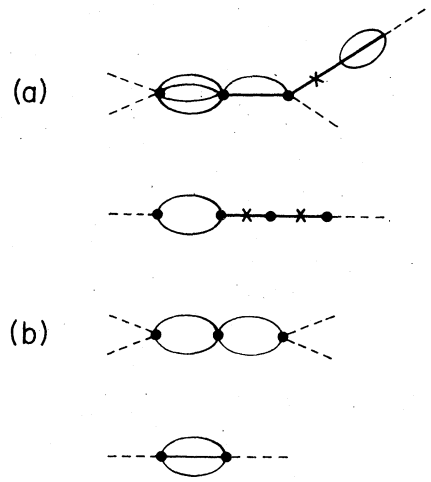

FIG. 10. (a) Reducible and (b) irreducible graphs. The graphs in (a) are reducible because they separate when the lines denoted by × are cut.

Generating functional for one-particle irreducible vertices

Let us recall that $\Gamma[\phi]$, the generating functional of one-particle-irreducible vertices, is defined via the Legendre transform

$$\Gamma[\phi] \equiv -\ln Z[J] + \int \phi(y)J(y)dy\,, \tag{4.1}$$

where the classical field $\phi(x)$ is defined by

$$\phi(x) \equiv \frac{\delta}{\delta J(x)}\ln Z[J] \quad (J \neq 0)\,, \tag{4.2}$$

and the vacuum persistence function $Z[J]$ is given in (1.1). Using (4.1) and (4.2) we can formally invert (4.2) to express J as a functional of the classical field ϕ:

$$J(x) = \frac{\delta\Gamma}{\delta\phi(x)}\,. \tag{4.3}$$

It is known[7] that Γ_n, defined by

$$\Gamma_n(x_1,\ldots,x_n)\equiv\frac{\delta}{\delta\phi(x_1)}\cdots\frac{\delta}{\delta\phi(x_n)}\Gamma[\phi]\,, \tag{4.4}$$

are the negatives of the exact one-particle-irreducible vertices of the full field theory, where here one-particle irreducibility refers to lines which represent the full two-particle Green's function W_2.

To understand the connection between the full Green's functions W_n and the one-particle-irreducible Green's functions Γ_n we consider the functional chain rule

$$\int dy\,\frac{\delta\phi(x)}{\delta J(y)}\,\frac{\delta J(y)}{\delta\phi(z)}=\delta(x-z)\,. \tag{4.5}$$

This equation tells us that W_2 and Γ_2 are inversely related:

$$W_2(x,y)=\Gamma_2(x,y)^{-1}\,. \tag{4.6}$$

Now we differentiate (4.6) with respect to $J(z)$:

$$W_3(x,y,z)=-\Gamma_3(a,b,c)W_2(x,a)W_2(y,b)W_2(z,c)\,, \tag{4.7}$$

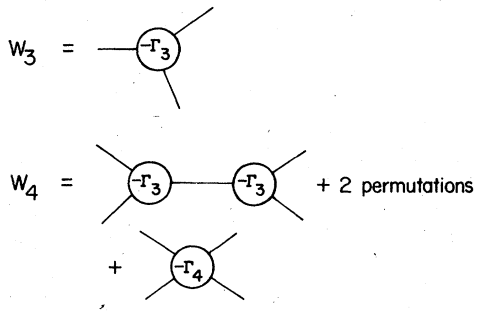

FIG. 11. The full n-point Green's functions W_n expressed diagrammatically in terms of the vertices $-\Gamma_n$ and the lines W_2. See (4.7) and (4.8).

where repeated arguments are integrated. This shows that Γ_3 is the one-particle-irreducible part of W_3 (see Fig. 11). (Γ_3 and W_3 vanish if we set $J=0$.) Next, we differentiate (4.7) with respect to J and use (4.6) and (4.7) to simplify the result

$$W_4(x,y,z,w)=-W_2(x,a)W_2(y,b)W_2(z,c)W_2(w,d)\Gamma_4(a,b,c,d)$$
$$+[W_2(x,a)W_2(y,b)\Gamma_3(a,b,e)W_2(e,f)\Gamma_3(f,c,d)W_2(c,z)W_2(d,w)+2\,\text{permutations}]\,. \tag{4.8}$$

Repeated differentiation with respect to J generates expressions for W_n in terms of $\Gamma_m(m\leq n)$ and W_2 and gives the interpretation of Γ_n as the one-particle-irreducible vertices. On the mass shell and when $J=0$, the Fourier transforms of Γ_{2n} are the $2n$-particle scattering amplitudes. It is easy to invert the equations for W_n in terms of Γ_n to express Γ_n in terms of W_n.

In weak-coupling perturbation theory it is easy to express $\Gamma_{2n}\big|_{J=0}$ in terms of one-particle-irreducible Feynman graphs, where the lines represent $[D(x,y)^{-1}+m^2\delta(x-y)]^{-1}$. However, in strong-coupling perturbation theory, where the lines of the graphs represent $D^{-1}(x,y)$, the natural quantities to calculate are the Λ_{2n} defined at the beginning of this section. Thus, the problem is to calculate Γ_{2n} in terms of Λ_{2n}.

We begin by expressing W_2 in terms of Λ_2. Since Λ_2 is the sum of all one-particle-irreducible graphs, we have

$$W_2=\Lambda_2+\Lambda_2D^{-1}\Lambda_2+\Lambda_2D^{-1}\Lambda_2D^{-1}\Lambda_2+\ldots$$
$$=\frac{\Lambda_2}{1-D^{-1}\Lambda_2}=\frac{1}{\Lambda_2^{-1}-D^{-1}}\,. \tag{4.9}$$

Thus, from (4.6)

$$\Gamma_2=-D^{-1}+\Lambda_2^{-1}\,, \tag{4.10a}$$

or in momentum space

$$\tilde{\Gamma}_2(p)=-p_M^{\,2}+\tilde{\Lambda}_2^{-1}(p)\,. \tag{4.10b}$$

So, $\tilde{\Lambda}_2^{-1}(p)$ is the vacuum polarization.

Next, we express W_4 in terms of the strong-coupling perturbation theory graphs. First, we have all one-particle-irreducible diagrams having four external legs. Next, we have all such diagrams with just one leg dressed with all possible one-particle-reducible graphs: $\Lambda_4(D^{-1}W_2)$. There are altogether four ways of doing this. Then we can dress two legs in six ways, three legs in four ways, and all four legs. Summing over all these possibilities gives

$$W_4=\Lambda_4(1+D^{-1}W_2)^4=\Lambda_4(W_2\Lambda_2^{-1})^4 \tag{4.11}$$

which, when written out explicitly, with integrations of the repeated arguments implied, is

$$W_4(x,y,z,w)=\Lambda_4(a,b,c,d)[\delta(a-x)+D^{-1}(a,e)W_2(e,x)][\delta(b-y)+D^{-1}(b,f)W_2(f,y)]$$
$$\times[\delta(c-z)+D^{-1}(c,g)W_2(g,z)][\delta(d-w)+D^{-1}(d,h)W_2(h,w)]\,.$$

Since $W_{2n+1}=0$ when $J=0$, (4.8) and (4.10) give

$$\Gamma_4 = -W_4(W_2^{-1})^4 = -\Lambda_4(\Lambda_2^{-1})^4 . \tag{4.12}$$

The next two expressions for Γ_6 and Γ_8 at $J=0$ in terms of W_{2n} are

$$\Gamma_6 = -W_6(W_2^{-1})^6 + 10(W_2^{-1})^3 W_4 W_2^{-1} W_4 (W_2^{-1})^3 \tag{4.13}$$

and

$$\Gamma_8 = -W_8(W_2^{-1})^8 + 56(W_2^{-1})^5 W_6 W_2^{-1} W_4 (W_2^{-1})^3 - 280(W_2^{-1})^3 W_4 W_2^{-1} W_4 (W_2^{-1})^2 W_2^{-1} W_4 (W_2^{-1})^3 . \tag{4.14}$$

In analogy with (4.11), we can express W_6 and W_8 in terms of Λ_{2n}:

$$W_6 = \Lambda_6(W_2\Lambda_2^{-1})^6 + 10(W_2\Lambda_2^{-1})^3\Lambda_4(D^{-1}+D^{-1}W_2D^{-1})\Lambda_4(W_2\Lambda_2^{-1})^3 \tag{4.15}$$

and

$$\begin{aligned} W_8 = {} & \Lambda_8(W_2\Lambda_2^{-1})^8 + 56(W_2\Lambda_2^{-1})^5\Lambda_6(D^{-1}+D^{-1}W_2D^{-1})\Lambda_4(W_2\Lambda_2^{-1})^3 \\ & + 280(W_2\Lambda_2^{-1})^3\Lambda_4(D^{-1}+D^{-1}W_2D^{-1})(W_2\Lambda_2^{-1})^2\Lambda_4(D^{-1}+D^{-1}W_2D^{-1})\Lambda_4(W_2\Lambda_2^{-1})^3 . \end{aligned} \tag{4.16}$$

Substituting (4.11), (4.15) and (4.16) into (4.13) and (4.14) gives expressions for Γ_{2n} in terms of Λ_{2n}:

$$\Gamma_6 = -\Lambda_6(\Lambda_2^{-1})^6 + 10(\Lambda_2^{-1})^6\Lambda_4\Lambda_2^{-1}\Lambda_4 \tag{4.17}$$

and

$$\begin{aligned} \Gamma_8 = {} & -\Lambda_8(\Lambda_2^{-1})^8 + 56(\Lambda_2^{-1})^8\Lambda_6\Lambda_2^{-1}\Lambda_4 \\ & - 280(\Lambda_2^{-1})^8\Lambda_4\Lambda_2^{-1}\Lambda_4\Lambda_2^{-1}\Lambda_4 . \end{aligned} \tag{4.18}$$

Note that the structure of (4.17) and (4.18) is the same as that in (4.13) and (4.14) with Λ_{2n} replacing W_{2n}. There is a graphical interpretation for Γ_{2n} in terms of Λ_{2n} (or W_{2n}) whose symmetry numbers yield the correct coefficients (see Fig. 12).

Effective potential

From (4.4) we can see that the functional $\Gamma(\phi)$ has a Taylor expansion in powers of ϕ at $\phi=0$:

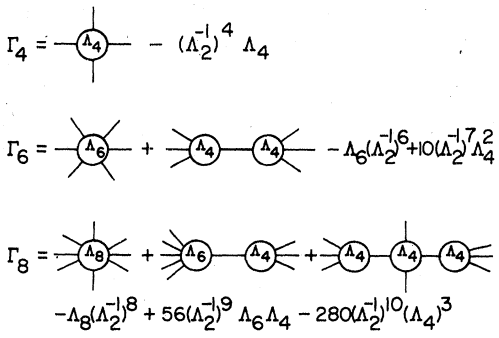

FIG. 12. Graphical representation of Γ_{2n} in terms of Λ_{2n}. Lines represent Λ_2^{-1} and vertices represent $-\Lambda_4$, $-\Lambda_6$, $-\Lambda_8$, $\cdots$. The factors 10, 56, 280, $\cdots$ are the symmetry numbers of the graphs. For example, $10 = 6!/(3!\,3!\,2!)$, $56 = 8!/(5!\,3!)$, $280 = 8!/(3!\,3!\,2!\,2!)$.

$$\Gamma[\phi] = \sum_{n=0}^{\infty}\frac{1}{(2n)!}\int dx_1\cdots dx_{2n}\,\Gamma_{2n}(x_1,\cdots,x_{2n}) \times \phi(x_1)\cdots\phi(x_{2n}) , \tag{4.19}$$

where we have used $\Gamma_{2n+1}(x_1,\ldots,x_{2n+1})=0$ at $J=0$. Now consider a source J which is constant and uniform in Euclidean space-time. This implies that ϕ is a constant independent of space-time. We define the Fourier transform of $\Gamma_{2n}(x_1,\ldots,x_{2n})$ by

$$\Gamma_{2n}(x_1,\ldots,x_{2n}) = \int \frac{dk_1}{(2\pi)^d}\cdots\frac{dk_{2n}}{(2\pi)^d}\exp\left(-i\sum_{i=1}^{2n}x_ik_i\right) \times\left[(2\pi)^d\delta\left(\sum_{i=1}^{2n}k_i\right)\tilde{\Gamma}_{2n}(k_1,\ldots,k_{2n})\right] . \tag{4.20}$$

Thus, for constant $\phi(x_i)=\phi$ we have

$$\begin{aligned} \Gamma(\phi) &= \sum_{n=0}^{\infty}\frac{1}{(2n)!}\tilde{\Gamma}_{2n}(0,0,0,\ldots,0)\phi^{2n}(2\pi)^d\delta(0) \\ &\equiv (2\pi)^d\delta(0)V(\phi) , \end{aligned} \tag{4.21}$$

which is the defining equation for the effective potential $V(\phi)$. Thus, the Taylor coefficients of the effective potential are the one-particle-irreducible vertices $\tilde{\Gamma}_{2n}(0,0,0,\ldots,0)$ evaluated at zero external momentum.

Alternative derivation of Taylor expansion for effective potential

For constant J and thus for constant ϕ (4.1) becomes

$$V(\phi)\Omega = -\ln Z(J) + \phi J\Omega , \tag{4.22}$$

where

$$\Omega=(2\pi)^d\delta(p)\big|_{p=0}$$

is the volume of space-time. Using

$$\phi=\frac{1}{\Omega}\frac{\partial}{\partial J}\ln Z\,, \tag{4.23}$$

it follows from (4.22) that

$$J=\frac{\partial V}{\partial\phi}\,. \tag{4.24}$$

For constant J, the path-integral representation of Z in (1.1) becomes

$$Z(J)=\int\mathfrak{D}\chi\exp\left[-\int d^dx\,\mathfrak{L}(\chi)+J\int\chi(x)dx\right], \tag{4.25}$$

where we integrate over the dummy function χ. To evaluate this integral we insert a representation for the number one in the integrand[10]:

$$1=\Omega\int\delta\left(\phi\Omega-\int\chi(x)dx\right)d\phi\,.$$

Thus,

$$Z(J)=\int d\phi\,e^{-\Omega[F(\phi)-\phi J]}\,, \tag{4.26}$$

where

$$e^{-F(\phi)\Omega}=\Omega\int\mathfrak{D}\chi\,\delta\left(\phi\Omega-\int\chi(x)dx\right)e^{-\int\mathfrak{L}(\chi)dx}\,. \tag{4.27}$$

Since the volume Ω of space-time is infinite we can evaluate (4.26) exactly by Laplace's method, keeping only the geometrical optics contribution to the leading term:

$$\ln Z(J)=-\Omega[F(\phi_0)-\phi_0J]+O(\ln\Omega)\,, \tag{4.28}$$

where ϕ_0 satisfies the stationarity condition

$$\frac{\partial F(\phi)}{\partial\phi}-J\bigg|_{\phi=\phi_0}=0\,. \tag{4.29}$$

Comparing (4.28) and (4.29) with (4.22) and (4.24) shows that as $\Omega\to\infty$, $F(\phi)$ in (4.26) and (4.27) can be identified with the effective potential V.

Next we evaluate (4.27) by using an integral representation for the δ function

$$e^{-V(\phi)\Omega}=\Omega\int\frac{dk}{2\pi}e^{-i\phi k\Omega}\int\mathfrak{D}\chi\exp\left\{-\int d^dx[\mathfrak{L}(\chi)+ik\chi]\right\} \tag{4.30}$$

and we recognize that the functional integral in (4.30) is just $Z[k]$ [see (1.1)]. But $\ln Z(k)$ has an expansion in terms of the connected Green's functions at zero external momentum $\tilde{W}_{2n}(p,p,p,\ldots,p)\big|_{p=0}$:

$$\ln Z(k)=\Omega\sum_{n=0}^{\infty}\frac{k^{2n}}{(2\pi)!}\tilde{W}_{2n}(0,0,0,\ldots,0)\,, \tag{4.31}$$

where

$$\tilde{W}_{2n}(p_1,p_2,\ldots,p_{2n})(2\pi)^d\delta\left(\sum_{i=1}^{2n}p_i\right)=\int dx_1\ldots\int dx_{2n}\exp\left(i\sum_{i=1}^{2n}x_ip_i\right)W(x_1,\ldots,x_{2n})\,.$$

Substituting (4.31) into (4.30) and replacing powers of k higher than quadratic by derivative operators gives

$$-V(\phi)=\lim_{\Omega\to\infty}\frac{1}{\Omega}\ln\left\{\exp\left[\sum_{n=2}^{\infty}\frac{1}{(2n)!}\tilde{W}_{2n}(0,0,\ldots,0)\Omega\left(\frac{1}{\Omega}\frac{\partial}{\partial\phi}\right)^{2n}\right]\times\exp[-\phi^2W_2^{-1}(0)\Omega/2]\right\}. \tag{4.32}$$

Expanding the right side of (4.32) and keeping terms which do not vanish as $\Omega\to\infty$ gives

$$V(\phi)=\sum_{n=0}^{\infty}\frac{V_{2n}}{(2n)!}\phi^{2n}\,, \tag{4.33}$$

where the coefficients V_{2n} are expressed in terms of the W_{2n} exactly as the Γ_{2n} are in (4.6), (4.12), (4.13), (4.14), and so on. This completes our alternative derivation of the relationship between the connected Green's functions W_{2n} and the coefficients of ϕ^{2n} in the effective potential.

Computation of $\tilde{\Lambda}_{2n}(p,p,\ldots,p)|_{p=0}$ in terms of OVIS's

We have shown how to express the coefficients of ϕ^{2n} in the effective potential in terms of sums of the one-particle-irreducible strong-coupling diagrams $\tilde{\Lambda}_{2n}(p,p,\ldots,p)\big|_{p=0}$. However, to evaluate a graph having $2n$ external legs at zero external momentum requires that we integrate each leg of the strong-coupling diagram over all space-time. This is equivalent to treating the original graph as a vacuum graph, which we have shown in Sec. III is a product of OVIS's.

Here is an example of how to evaluate a graph contributing to $\tilde{\Lambda}_6(0,0,0,\ldots,0)$. Consider the seven-internal-line one-particle-irreducible graph in Fig. 13(a). The external-symmetry number for

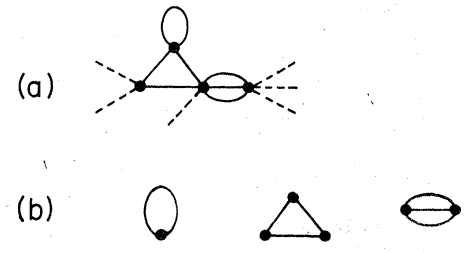

FIG. 13. (a) A one-particle-irreducible graph contributing to $\tilde{\Lambda}_6(0,0,\cdots,0)$ and (b) its decomposition into a product of vacuum OVIS's.

TABLE I. Number of one-particle-irreducible graphs in Λ_2, Λ_4, Λ_6, and Λ_8 vs the number of internal lines. We have evaluated all of these graphs.

Number of internal lines	Number of graphs in Λ_2	Number of graphs in Λ_4	Number of graphs in Λ_6	Number of graphs in Λ_8
0	1	1	1	1
1	1	1	1	1
2	2	3	3	4
3	5	7	10	12
4	12	23	32	48
5	34	67	116	
6	97	240		
7	100[a]			

[a]Graphs having p^2 dependence only.

this graph (involving permutations of the external legs) is 60. The internal-symmetry number (involving permutations of the internal lines) is $\frac{1}{12}$. The vertices are $L_4^2 L_6^2$. In Fig. 13(b) the graph is decomposed into its OVIS's, which are evaluated in Fig. 7 as $(-2d)a^{-d-2}$, $(-12d^2 - 8d^3)a^{-d-6}$, and $(2d - 8d^3)a^{-2d-6}$. To obtain the contribution of this graph to Λ_6 we multiply together the external and internal symmetry numbers, the vertices, and the values of the OVIS's.

In Table I we list the number of graphs contributing to Λ_2, Λ_4, Λ_6, and Λ_8 versus the number of internal lines. We have evaluated all of these graphs.

This completes our discussion of the evaluation of the unrenormalized effective potential.

Wave-function renormalization of the effective potential

In this paper we follow an intermediate renormalization scheme in which we define the wave-function-renormalization constant Z at $p = 0$:

$$Z^{-1} \equiv -\frac{\partial W_2^{-1}}{\partial (p_M^2)}\bigg|_{p_M^2=0} = 1 - \frac{\partial}{\partial (p_M^2)} \tilde{\Lambda}_2^{-1}(p_M)\bigg|_{p_M=0}. \tag{4.34}$$

This means that we must know the momentum dependence of $\tilde{\Lambda}_2$. We have already given in Sec. III a detailed discussion of how to find the p^2 dependence of the propagator graphs.

Given Z, we simultaneously renormalize the coefficients of the effective potential V and the classical field ϕ by defining

$$\phi^R \equiv \frac{1}{\sqrt{Z}}\,\phi \tag{4.35}$$

and

$$\tilde{\Gamma}_{2n}^R(0,0,\ldots,0) = Z^n \tilde{\Gamma}_{2n}(0,0,\ldots,0). \tag{4.36}$$

Note that reexpressing V in terms of these renormalized quantities leaves V unchanged.

$$V = \sum_{n=0}^{\infty} \frac{(\phi^R)^{2n}}{(2n)!} \tilde{\Gamma}_{2n}^R(0,0,\ldots,0). \tag{4.37}$$

In this intermediate renormalization scheme, the renormalized mass M and the renormalized coupling constant G are given in terms of the coefficients of V:

$$M^2 \equiv \tilde{\Gamma}_2^R(0,0) \tag{4.38}$$

and

$$G \equiv 24 \tilde{\Gamma}_4^R(0,0,0,0). \tag{4.39}$$

We also define dimensionless renormalized zero-momentum scattering amplitudes γ_{2n} by

$$\gamma_{2n} \equiv \tilde{\Gamma}_{2n}^R(0,0,\ldots,0) M^{nd-2n-d}, \quad \tilde{G} \equiv 24\gamma_4. \tag{4.40}$$

Corresponding to each of the two methods discussed in Sec. II for expanding the vertices, there is an expansion for M^2, γ_4, γ_6, γ_8, and Z. We conclude this paper by listing the first few orders in these expansions.

Method I (m^2 fixed).

$$M^2 a^2 \epsilon = (2R)^{-1} - (12dR^2 - d)\epsilon/(4R^2) + [(2d-1)144R^4 + (-2d^2 - d + 1)24R^2 + 6d^2 - 1]\epsilon^2/(48R^3) - (4R^2 - 1)s\epsilon/(8R^2) - (8R^2 - 1)ds\epsilon^2/(8R^3) - (8R^2 - 1)s^2\epsilon^2/(32R^3) + \cdots, \tag{4.41a}$$

$$\epsilon^2(2R\epsilon)^{d/2-2}\gamma_4=(12R^2-1)/(384R^4)-[(144d^2-384d)R^4-24d^2R^2+d^2+4d]\epsilon/(1536R^5)$$
$$+[(5184d^4-38\,016d^3+80\,640d^2-63\,360d)R^6+(-1296d^4+3744d^3-6912d^2+7776d)R^4$$
$$+(108d^4+312d^3+432d^2-168d)R^2-3d^4-30d^3-72d^2+2d]\epsilon^2/(36\,864R^6)$$
$$-[48dR^4-(d-2)16R^2+d+4]s\epsilon/(3072R^5)$$
$$+[(576d^3-2688d^2+3072d)R^6+(-240d^3+96d^2-384d)R^4$$
$$+(28d^3+120d^2+192d)R^2-d^3-10d^2-24d)]s\epsilon^2/(12\,288R^6)$$
$$+[(d-2)192dR^6+(-112d^2-416d-384)R^4+(20d^2+136d+256)R^2$$
$$-d^2-10d-24]s^2\epsilon^2/(49\,152R^6)+\cdots, \tag{4.41b}$$

$$\epsilon^3(2R\epsilon)^{d-3}\gamma_6=(480R^4-96R^2+5)/(46\,080R^7)$$
$$-[(5760d^2-11\,520d)R^6+(-1632d^2+816d)R^4+(156d^2+228d)R^2-5d^2-20d)]\epsilon/(92\,160R^8)$$
$$+[(20\,7360d^4-1\,036\,800d^3+1\,520\,640d^2-552\,960d)R^8$$
$$+(-76\,032d^4+180\,864d^3-196\,992d^2+165\,888d)R^6+(10\,512d^4+8496d^3+10\,080d^2-15\,312d)R^4$$
$$+(-648d^4-2976d^3-3456d^2+456d)R^2+15d^4+135d^3+300d^2-5d]\epsilon^2/(1\,105\,920R^9)$$
$$-[1920dR^6-(864d+1488)R^4+(d+3)116R^2-5d-20]s\epsilon/(184\,320R^8)$$
$$+[(23\,040d^3-69\,120d^2+46\,080d)R^8+(-12\,288d^3+1536d^2+6144d)R^6$$
$$+(2256d^3+6000d^2+3840d)R^4-(176d^3+992d^2+1472d)R^2+5d^3+45d^2+100d]s\epsilon^2/(368\,640R^9)$$
$$+[(d-1)7680dR^8-(5376d^2+14\,208d+8832)R^6+(1328d^2+6928d+9408)R^4$$
$$-(136d^2+992d+1832)R^2+5d^2+45d+100]s^2\epsilon^2/(1\,474\,560R^9)+\cdots, \tag{4.41c}$$

$$\epsilon^4(2R\epsilon)^{3d/2-4}\gamma_8=(25\,200R^6-8400R^4+939R^2-35)/(5\,160\,960R^{10})$$
$$-[(302\,400d^2-537\,600d)R^8+(-126\,000d^2+94\,080d)R^6+(19\,668d^2+10\,384d)R^4$$
$$-(1359d^2+2840d)R^2+35d^2+140d]\epsilon/(6\,881\,280R^{11})$$
$$+[(32\,659\,200d^4-137\,894\,400d^3+169\,344\,000d^2-49\,835\,520d)R^{10}$$
$$+(-16\,329\,600d^4+38\,465\,280d^3-34\,433\,280d^2+21\,692\,160d)R^8$$
$$+(3\,258\,144d^4-513\,792d^3+1\,729\,728d^2-3\,440\,448d)R^6$$
$$+(-323\,784d^4-775\,440d^3-516\,432d^2+239\,376d)R^4$$
$$+(16\,011d^4+85\,314d^3+110\,400d^2-6918d)R^2$$
$$-315d^4-2730d^3-5880d^2+70d]\epsilon^2/(165\,150\,720R^{12})$$
$$-[302\,400dR^8-(176\,400d+255\,360)R^6+(36\,468d+91\,248)R^4$$
$$-(3237d+10\,760)R^2+105d+420]s\epsilon/(41\,287\,680R^{11})$$
$$+[(10\,886\,400d^3-26\,611\,200d^2+12\,902\,400d)R^{10}+(-7\,257\,600d^3+1\,451\,520d^2+5\,806\,080d)R^8$$
$$+(1\,842\,048d^3+3\,458\,880d^2+261\,888d)R^6-(225\,936d^3+897\,120d^2+822\,528d)R^4$$
$$+(13\,491d^3+83\,634d^2+131\,120d)R^2-315d^3-2730d^2-5880d]s\epsilon^2/(165\,150\,720R^{12})$$
$$+[(3\,628\,800d^2-2\,419\,200d)R^{10}-(3\,024\,000d^2+6\,531\,840d+3\,010\,560)R^8$$
$$+(966\,816d^2+4\,186\,368d+4\,545\,792)R^6-(148\,248d^2+897\,840d+1\,373\,056)R^4$$
$$+(10\,971d^2+81\,954d+153\,520)R^2-315d^2-2730d-5880]s^2\epsilon^2/(660\,602\,880R^{12})+\cdots, \tag{4.41d}$$

$$Z=1-(144R^4-24R^2+1)\epsilon^2/(24R^2)-[1152dR^6-96dR^4-24dR^2+2d]\epsilon^3/(48R^3)$$
$$-[(414\,720d^2+552\,960d-760\,320)R^8+(-23\,040d^2-115\,200d+138\,240)R^6$$
$$+(5760d^2+11\,520d-10\,368)R^4+(-2400d^2-480d+480)R^2+180d^2-10]\epsilon^4/(5760R^4)$$
$$-[576R^6-48R^4-12R^2+1]s\epsilon^3/(48R^3)-[414\,720dR^8-23\,040dR^6+5760dR^4-2400dR^2+180d]s\epsilon^4/(5760R^4)$$
$$-[103\,680R^8-5760R^6+1440R^4-600R^2+45]s^2\epsilon^4/(5760R^4)+\cdots. \tag{4.41e}$$

Method II (m^2 large and negative).

$$M^2a^2=\alpha^{-1}-2d+(6d-2)\alpha/3+(180d^2-390d+194)\alpha^3/45+(30\,240d^3-124\,740d^2+162\,792d-68\,164)\alpha^5/945$$
$$+[\alpha^{-1}+2d+(-4d+2)\alpha-(12d^2-4d)\alpha^2/3-(540d^2-1560d+914)\alpha^3/45-(1080d^3-2340d^2+1564d-360)\alpha^4/45$$
$$-(151\,200d^3-703\,920d^2+998\,004d-445\,028)\alpha^5/945]\delta$$
$$+[4\alpha^{-1}+6d+(4d^2-10d+4)\alpha+(-8d^2+4d)\alpha^2+(-24d^2+48d-22)\alpha^3+(360d^3-1040d^2+1036d-360)\alpha^4/15$$
$$+(45\,360d^4-257\,040d^3+542\,388d^2-450\,660d+112\,874)\alpha^5/945]\delta^2$$
$$+[31\alpha^{-1}+40d+(72d^2-228d+94)\alpha/3+(8d^3-60d^2+24d)\alpha^2-(720d^3+9360d^2-22\,740d+11\,792)\alpha^3/45$$
$$-(432d^3-864d^2+284d+72)\alpha^4/9-(100\,800d^3-413\,880d^2+537\,896d-224\,218)\alpha^5/45]\delta^3+\cdots, \tag{4.42a}$$

$$\alpha^{d/2}\tilde{G}=2-(2d^2-8d)\alpha+(3d^4-30d^3+78d^2-62d)\alpha^2/3-(d^6-18d^5+110d^4-290d^3+300d^2-112d)\alpha^3/3$$
$$+(15d^8-420d^7+4440d^6-22\,860d^5+59\,340d^4-73\,440d^3+25\,820d^2+6736d)\alpha^4/180$$
$$-(3d^{10}-120d^9+1920d^8-15\,980d^7+74\,292d^6-192\,400d^5+250\,460d^4-110\,304d^3-71\,216d^2+63\,168d)\alpha^5/180$$
$$+[d-2-(d^3-10d^2+16d)\alpha+(3d^5-60d^4+330d^3-638d^2+452d)\alpha^2/6$$
$$+(d^7-32d^6+338d^5-1578d^4+3520d^3-3440d^2+1216d)\alpha^3/6$$
$$+(15d^9-690d^8+11\,520d^7-93\,780d^6+409\,380d^5-960\,360d^4+1\,120\,460d^3-450\,104d^2-39\,456d)\alpha^4/360$$
$$-(3d^{11}-186d^{10}+4440d^9-54\,740d^8+386\,492d^7-1\,609\,384d^6+3\,872\,460d^5-4\,892\,504d^4$$
$$+2\,256\,784d^3+934\,592d^2-898\,368d)\alpha^5/360]\delta$$
$$+[(d^2+10d-24)/4-(d^4-2d^3-72d^2+192d)\alpha/4+(3d^6-48d^5+42d^4+1558d^3-4476d^2+3152d)\alpha^2/24$$
$$-(d^8-32d^7+314d^6-846d^5-1688d^4+10\,104d^3-12\,480d^2+4224d)\alpha^3/24$$
$$+(15d^{10}-750d^9+13\,800d^8-118\,380d^7+509\,940d^6-1\,084\,200d^5+970\,940d^4$$
$$-205\,624d^3+455\,552d^2-554\,304d)\alpha^4/1440$$
$$+(3d^{12}-210d^{11}+5808d^{10}-82\,940d^9+680\,892d^8-3\,377\,000d^7+10\,278\,332d^6-18\,979\,784d^5$$
$$+20\,310\,608d^4-10\,552\,864d^3+1\,415\,424d^2+186\,624d)\alpha^5/1440]\delta^2$$
$$+[(d^3+36d^2+500d-960)/24-(d^5+20d^4+140d^3-3632d^2+8448d)\alpha/24$$
$$+(3d^7+6d^6-78d^5-10\,922d^4+100\,320d^3-242\,632d^2+166\,848d)\alpha^2/144$$
$$-(d^9-18d^8+106d^7-3254d^6+58\,324d^5-371\,408d^4+962\,976d^3-987\,392d^2+342\,528d)\alpha^3/144$$
$$+(15d^{11}-600d^{10}+9780d^9-120\,900d^8+1\,585\,260d^7-14\,862\,960d^6+76\,041\,500d^5-198\,277\,904d^4$$
$$+243\,615\,184d^3-86\,053\,888d^2-21\,468\,288d)\alpha^4/8640$$
$$-(3d^{13}-192d^{12}+5220d^{11}-84\,260d^{10}+989\,412d^9-9\,141\,248d^8+61\,051\,580d^7-261\,706\,064d^6$$
$$+656\,565\,536d^5-842\,837\,664d^4+362\,260\,544d^3+241\,400\,448d^2-208\,392\,192d)\alpha^5/8640]\delta^3+\cdots, \tag{4.42b}$$

$$\alpha^d\gamma_6=(\tfrac{1}{30})-(d^2-3d)\alpha/15+(3d^4-21d^3+39d^2-10d)\alpha^2/45-(4d^6-12d^5+50d^4-82d^3+40d^2+12d)\alpha^3/90$$
$$+(15d^8-270d^7+1875d^6-6240d^5+9945d^4-5535d^3-430d^2+992d)\alpha^4/675$$
$$-(6d^{10}-150d^9+1530d^8-8150d^7+24\,054d^6-37\,360d^5+25\,150d^4-1126d^3+6864d^2-10\,458d)\alpha^5/675+\cdots, \tag{4.42c}$$

$$\alpha^{3d/2}\gamma_\delta=(\tfrac{1}{56})-(3d^2-8d)\alpha/56+(9d^4-54d^3+86d^2-18d)\alpha^2/112$$
$$-(27d^6-270d^5+942d^4-1302d^3+540d^2-32d)\alpha^3/336+\cdots, \quad (4.42d)$$
$$Z=1-2\alpha^2/3-(180d-194)\alpha^4/45+[8\alpha^2/3+8d\alpha^3/3+(960d-1108)\alpha^4/45+(1440d^2-1952d+360)\alpha^5/45]\delta$$
$$+[4\alpha^2-(120d^2-660d+658)\alpha^4/45-(3840d^2-6112d+1440)\alpha^5/45]\delta^2$$
$$+[112\alpha^2/3+16d\alpha^3+(11\,520d-12\,716)\alpha^4/45+(32d-24)\alpha^5/3]\delta^3+\cdots. \quad (4.42e)$$

The mass renormalization of these expressions is discussed in the next paper of this series.

ACKNOWLEDGMENTS

We thank the MIT MATHLAB group for the use of MACSYMA. One of us (G.S.G) would also like to thank the Brown University Materials Research Laboratory for partial support under its NSF grant. R. R. thanks the NSF and the rest of us thank the DOE for financial support for this project.

APPENDIX

In this appendix, we relate our expansion method to the more traditional high-temperature expansion used in statistical mechanics. The conversion enables us to check our results against existing series,[11] and to extend our results to ten internal lines for two, three, and four dimensions.

Both approaches begin with the generating functional on a d-dimensional lattice

$$Z[J]=\int[\mathfrak{D}\phi]\exp\left(\sum_i a^d\,\frac{\phi_i(\phi_{i+1}+\phi_{i-1}-2d\phi_i)}{2a^2}-V(\phi_i)-J_i\phi_i\right), \quad (A1)$$

where $V(\phi_i)$ is the potential, and involves only ϕ_i and not ϕ at neighboring sites. We proceed by extracting the full kinetic energy term to obtain

$$Z[J]=\exp\left(\sum_i v\,\frac{1}{2}\,\frac{\delta}{\delta J_i}\,\frac{\delta}{\delta J_{i+1}}+\frac{\delta}{\delta J_{i-1}}-2d\,\frac{\delta}{\delta J_i}\right)$$
$$\times\int[\mathfrak{D}\phi]\exp\left(-\sum_i a^d[V(\phi_i)+J_i\phi_i]\right) \quad (A2)$$

with

$$v=a^{-(d+2)}. \quad (A3)$$

The remaining functional integral is a product of ordinary integrals at each space-time point. The vertices L_{an} of our theory are obtained from

$$\frac{\int d\phi\, e^{-a^d[V(\phi)+J\phi]}}{\int d\phi\, e^{-a^d V(\phi)}}=\exp\left(\sum_n L_{2n}J^{2n}/(2n)!\right). \quad (A4)$$

[We have assumed that $V(\phi)$ is an even function.]

In the usual high-temperature series expansion, only the "off-diagonal" piece of the kinetic energy term is extracted, so that

$$Z[J]=\exp\left(\sum_i v\,\frac{1}{2}\,\frac{\delta}{\delta J_i}\,\frac{\delta}{\delta J_{i+1}}+\frac{\delta}{\delta J_{i-1}}\right)$$
$$\times\int[\mathfrak{D}\phi]\exp\left\{-\sum_i a^d\left[V(\phi_i)+J_i\phi_i+\frac{d}{a^2}\phi_i^2\right]\right\}. \quad (A5)$$

The moments I_n of the high-temperature expansion are defined by

$$\frac{\int d\phi\exp\{-a^d[V(\phi)+d\phi^2/a^2+J\phi]\}}{\int d\phi\exp\{-a^d[V(\phi)+d\phi^2/a^2]\}}=\sum\frac{J^{2n}I_{2n}}{(2n)!}. \quad (A6)$$

Note that in both cases, v counts propagator insertions, or the number of lines in the diagram. The high-temperature series propagator has no diagonal piece, so that there are no graphs with loops (lines beginning and ending at the same vertex). This reduces the number of graphs significantly. Our propagator has a diagonal piece, but the sum of its numerical coefficients vanishes, which means that there are no tadpoles (see Fig. 14).

The relationship between the I_{2n} and L_{2n} is more easily obtained by defining

$$x=\phi a^d$$

and

$$a^d V(x)=V_1(x), \quad (A7)$$

so that

$$\exp\left[\sum_n L_{2n}J^{2n}/(2n)!\right]=\frac{\int dx\, e^{-Jx-V_1(x)}}{\int dx\, e^{-V_1(x)}} \quad (A8)$$

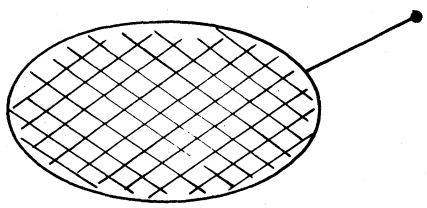

FIG. 14. A tadpole graph where the shaded area represents any graph, and the free vertex is to be summed over.

and

$$\sum_n I_{2n} J^{2n}/(2n)! = \frac{\int dx\, e^{-Jx - V_1(x) - dvx^2}}{\int dx\, e^{-V_1(x) - dvx^2}}. \quad \text{(A9)}$$

Let

$$I'_{2n} = \frac{\int x^{2n} e^{-V_1(x)} dx}{\int e^{-V_1(x)} dx}; \quad \text{(A10)}$$

then

$$\exp\left(\sum_n L_{2n} J^{2n}/(2n)!\right) = \sum_p I'_{2p} J^{2p}/(2p)! \quad \text{(A11)}$$

and

$$I_{2n} = \frac{\sum_p [(-dv)^p/p!] I'_{2n+2p}}{\sum_p [(-dv)^p/p!] I'_{2p}}. \quad \text{(A12)}$$

We solve for I' in terms of L from (A11), and for I in terms of I' from (A12). Since v counts propagator lines and we only work to a given number of lines, it is sufficient to expand (A12) to a given order in v.

The easiest way to compute the relation between I'_{2p} and L_{2n} is to differentiate both sides of (A11) with respect to J, obtaining

$$\sum_n \frac{L_{2n} J^{2n-1}}{(2n-1)!} \sum_p \frac{I'_{2p} J^{2p}}{(2p)!} = \sum_q \frac{I'_{2q} J^{2q-1}}{(2q-1)!} \quad \text{(A13)}$$

or

$$\frac{I'_{2q}}{(2q-1)!} = \sum_{n=1}^{q} \frac{L_{2n}}{(2n-1)!} \frac{I'_{2q-2n}}{(2q-2n)!}. \quad \text{(A14)}$$

If we write

$$I_{2n} = \sum_{q=0}^{\infty} J_{2n,q} (-dv)^q, \quad \text{(A15)}$$

then cross multiplying (A12) yields

$$J_{2n,r} = \frac{I'_{2n+2r}}{r!} - \sum_{q=0}^{r-1} J_{2n,q} \frac{I'_{2r-2q}}{(r-q)!}. \quad \text{(A16)}$$

Because I_{2n} is explicitly a power series in v, reconstruction of the high-temperature results for N lines requires our results for 1 up to N lines, and vice versa.

---

*Permanent address: Physics Department, Brown University, Providence, Rhode Island 02912.

[1]C. M. Bender, F. Cooper, G. S. Guralnik, H. Moreno, R. Roskies, and D. H. Sharp, Phys. Rev. Lett. 45, 501 (1980).

[2]C. M. Bender, F. Cooper, G. S. Guralnik, and D. H. Sharp, Phys. Rev. D 19, 1865 (1979). See also, P. Castoldi and C. Schomblond, Nucl. Phys. B139, 26 (1978); H. Kaiser, Zeuthen Report No. PHE7411, 1974 (unpublished).

[3]C. M. Bender, F. Cooper, G. S. Guralnik, R. Roskies, and D. H. Sharp, in Proceedings of the Orbis Scientiae Conference—1980, edited by Arnold Perlmutter (to be published). Invited talk given by F. Cooper. This reference contains earlier historical references on the strong-coupling expansion.

[4]C. M. Bender, F. Cooper, and G. S. Guralnik, Ann. Phys. (N.Y.) 109, 165 (1977).

[5]G. A. Baker and J. M. Kincaid, Phys. Rev. Lett. 42, 1431 (1979) and unpublished.

[6]A less-refined version of this notation was introduced in Ref. 2.

[7]B. Nickel, private communication.

[8]On the lattice the Fourier transform of the second difference operator is $2[\cos(pa) - 1]/a^2$. In what follows we understand that $-p^2$ stands for this expression. In this paper the distinction between the two is irrelevant since we only compute to order p^2.

[9]For a review of functional methods in quantum field theory and the effective potential, see J. Iliopoulos, C. Itzykson, and A. Martin, Rev. Mod. Phys. 47, 165 (1975).

[10]See R. Brout, in *Lecture Notes in Physics 54, Critical Phenomena,* Sitges International School on Statistical Mechanics, edited by J. Brey and R. B. Jones (Springer, Berlin, 1976), p. 354.

[11]See, e.g., J. P. Van Dyke and W. J. Camp, Phys. Rev. Lett. 35, 323 (1975), or J. M. Kincaid, G. A. Baker, and L. W. Fullerton, Los Alamos Report No. LA-UR-79-1575 1979 (unpublished).